2015

DEPARTAMENTO DE CIÊNCIAS DA VIDA

FACULDADE DE CIÊNCIAS E TECNOLOGIA
UNIVERSIDADE DE COIMBRA

Dissociating the role of interneurons in sensory procesing

Dissociating the role of interneurons in sensory processing

Inês Vitória Barreiros

Inês Vitória Barreiros

2015

DEPARTAMENTO DE CIÊNCIAS DA VIDA

FACULDADE DE CIÊNCIAS E TECNOLOGIA
UNIVERSIDADE DE COIMBRA

Dissociating the role of interneurons in sensory processing

Dissertação apresentada à Universidade de Coimbra para cumprimento dos requisitos necessários à obtenção do grau de Mestre em Biologia Celular e Molecular, realizada sob a orientação científica do Doutor Michael Kohl (Universidade de Oxford, Reino Unido) e sob co-orientação do Professor Carlos B. Duarte (Universidade de Coimbra, Portugal).

Inês Vitória Barreiros

2015

The work described in this thesis was performed at the Department of Physiology, Anatomy and Genetics, University of Oxford, United Kingdom with support from the ERASMUS+ Programme.

À minha mãe, Leonilde,

a minha maior inspiração.

If the doors of perception were cleansed everything would appear to man as it is, Infinite.
William Blake

Acknowledgements

This thesis symbolises an important stage in both my education and my scientific career. It represents not only the conclusion of my master degree but also the moment in which I accomplish one of my biggest dreams by experiencing the feeling of becoming a real neuroscientist!

A number of people contributed to the success of the work described in this thesis either by helpful collaborations or invaluable support and friendship. Thus, I would like to take this opportunity to express my deepest gratitude to:

My supervisor, Dr. Michael Kohl, for accepting me as part of his research group and giving me the opportunity to work on such an interesting and exciting project. For the adventure of participating on the setting up of a new lab and group in such an amazing place as Oxford and for giving me opportunity to continue here. For all the knowledge transmitted throughout this year and for encouraging me to be an independent researcher. For supporting me, having faith in my capacities and inspiring me to follow my dreams. In sum, thank you for being much more than an amazing supervisor: a great mentor and a good friend!

My internal tutor, Professor Carlos Duarte (University of Coimbra), for accepting this role on my thesis and being always prompt to answering my questions. For all the knowledge transmitted during the first year of the master. Not only the scientific concepts, but for teaching us how to think as real scientists and inspiring us to work had and do good science!

My group colleagues Marta Huelin Gorriz and Ana Carolina Barros for the great invaluable teamwork, for the wonderful collaboration throughout this project and the interesting scientific and non-scientific discussions. For the amazing friendship and for so many great unforgettable moments! Thank you for, together with Michael, making of our lab, home, and of our group, a true family!

Oriol Pavón (Miesenböck's Group, DPAG), Professor Ed Mann (DPAG) and his students Pantelis Antonoudiou and Emanuel Oliveira for initiating me to the electrophysiology world and giving me advice on how to learn and deal with such a complex but precious technique!

Sebastian Vásquez-López and Mariangela Panniello (King's Group, DPAG) for all the kind help and advice on two-photon imaging experiments. And to Dr Mahesh Karnani (Yuste's Group, Columbia University, USA) for prompt advice on data analysis and helpful scientific discussions!

Dr Dennis Kaetzel (Department of Experimental Psychology) and Professor Colin Akerman (Department of Pharmacology) for kindly providing the transgenic mice strains essential to the development of this project.

My mother, Leonilde, for being my greatest inspiration with her astonishing passion for science and for the understanding of the brain mysteries. For, together with my brothers, Marco and André, encouraging me to follow my dreams by supporting me with such an unconditional love capable of crossing any borders!

In last but not least, to David Brito, for all the help, advice and support. For, despite of being at thousands of kilometres of distance, being so indispensable and present in all the important moments of my life, always making me smile, no matter what! Thank you for giving another meaning to the word 'friendship' by being the best friend one could ever dream of having!

Table of Contents

List of Figures

List of Tables

Abbreviations & Symbols

Ø	Diameter.
~	Approximately.
a.m.	Before midday.
AAV	Adenoassociated virus.
aCSF	Artificial cerebrospinal fluid.
AMCA	Aminomethylcoumarin.
AP	Anteroposterior.
AP	Action potential.
ATP	Adenosine triphosphate.
bp	Base pair.
ChR2	Channelrhodopsin 2.
ddH_2O	Deionized water.
DIO	Double-floxed inverted.
DNA	Deoxyribonucleic acid.
DPAG	Department of Physiology, Anatomy and Genetics.
E/I balance	Excitatory/Inhibitory balance.
EC	External capsule.
EDTA	Ethylenediamine tetraacetic acid.
EF1α	Elongation Factor 1α.
EPSPs	Excitatory post-synaptic potentials.
ES	Early spiking.
et al.	And others.
Exc.	Excitatory.
F0	Baseline fluorescence.
F1	First filial generation.
F2	Second filial generation.
Fim	Fimbria.
FS	Fast spiking.
GABA	γ-aminobutyric acid
GCaMP	Green fluorescent protein moiety attached to the calcium-binding protein calmodulin.

GCaMP6f	Fast version of the genetically encoded calcium indicator GCAMP6.
GTP	Guanosine-5'-triphosphate.
h	Hour.
hChR2	Humanized version of ChR2.
Hip	Hippocampus.
Hz	Hertz.
IC	Internal capsule.
INs	Interneurons.
IRES	Internal ribosome entry site.
Kb	Kilobases.
kg	Kilogram.
kHz	Kilohertz.
L	Liter.
L1	Layer 1.
L2/3	Layer 2/3.
L4	Layer 4.
L5	Layer 5.
L6	Layer 6.
LED	Light-emitting diode.
LS	Late spiking.
M	Molar concentration.
M1	Motor cortex.
mA	Miliampere.
mg	Milligram.
mHz	Megahertz.
min	Minute.
mL	Millilitre.
ML	Mediolateral.
mm	Millimetre.
mM	Millimolar.
mOsm	Milliosmole.
mV	Millivolt.
MW	Megawatt.

mW	Milliwatt.
MΩ	Megaohm.
NA	Numerical aperture.
NFSA	Non-fast spiking slow adapting.
ng	Nanogram.
nl	Nanolitre.
nm	Nanometre.
ns	Non-significant.
^{o}C	Celsius.
p	P-value.
P	Parental generation.
P [number]	Postnatal day.
pA	Picoamperes.
PBS	Phosphate buffered saline.
PCR	Polymerase chain reaction.
PFA	Paraformaldehyde.
POm	Posterior thalamic nucleus.
PV	Parvalbumin.
ROIs	Regions of interest.
RT	Room temperature.
RTN	Reticular thalamic nucleus.
s	Second.
S1	Primary somatosensory cortex.
S2	Secondary somatosensory cortex.
SD	Standard deviation.
SEM	Standard error of the mean.
Sst	Somatostatin.
Str	Striatum.
SV40	Simian vacuolating virus 40.
Syn	Synapsin I promotor.
TG	Trigeminal ganglia.
TN	Trigeminal nuclei.
UK	United Kingdom.

USA	United States of America.
VB	Ventrobasal nucleus.
vg	Vector genomes.
Vm	Membrane potential.
VMP	Ventral posterior nucleus.
vS1	Vibrissal somatosensory system.
WPRE	Woodchuck Hepatitis Virus Posttranscriptional Regulatory Element.
WT	Wild-type.
wt.	Weight percent.
ΔF	Delta fluorescence.
µA	Microampere.
µl	Microliter.
µm	Micrometre.
µs	Microsecond.

Abstract

There are a number of studies supporting both a rate and a temporal neural coding strategies. Whether information is encoded in the brain by one or the other is a hotly debated open question in the field of neuroscience. Both coding schemes seem to be involved in the processing of different features of a same stimulus. Therefore, it is likely they dynamically coexist in the brain. In both strategies, a balance between excitation and inhibition (E/I) and its necessary synchronous neuronal activity are critical for an adequate processing of sensory information.

Inhibition seems to have a particularly important role in these processes. Thus, it is important to take into account the diversity of inhibitory neuronal populations and their distinct characteristics, leading us to hypothesise that different classes of interneurons are involved in the regulation of activity-dependent transmission of different stimuli features by shifting processing of information towards a temporal or rate code.

In this project, in order to elucidate the proposed mechanisms, I combined optogenetic tools with *in vitro* electrophysiology recordings and *in vivo* two-photon calcium imaging of neural activity in the mouse barrel cortex. By combining cell-type specific expression of optogenetic actuators with optogenetic reporters, I established a methodological approach to dissect the role of inhibitory neurons in sensory processing.

Results obtained *in vitro* revealed a distinct role on the inhibition provided by Stt^+ and PV^+ inhibitory neurons during synaptic transmission of thalamocortical inputs. *In vivo* experiments support electrophysiological results by suggesting a close relation between PV^+ interneurons and excitatory cells activity during sensory processing. These results are in accordance with my initial hypothesis that cortical interneurons subpopulations have distinct roles in maintaining the balance between excitation and inhibition during sensory processing. This will guide further studies into the relative contribution of interneurons subpopulations for the coding strategies used in somatosensoryprocessing.

Keywords: barrel cortex, E/I balance, interneurons diversity, neural code, somatosensory processing.

Resumo

Existe um grande número de estudos a suportar a existência de ambas as estratégias de codificação neuronal baseadas na frequência ou no *timing* de potenciais de ação. Se informação é codificada no cérebro através de uma ou de outra, é atualmente uma questão em acesa discussão na área das neurociências. Ambas as estratégias de codificação parecem estar envolvidas no processamento de diferentes aspetos de um mesmo estímulo. Assim, é provável que elas coexistam no cérebro através de uma interação dinâmica. Em ambas, o balanço entre excitação e inibição (E/I) e a sua necessária de atividade neuronal sincronizada são aspetos críticos para um correto processamento de informação sensorial.

A inibição parece ter um papel particularmente importante nestes processos. Assim, é importante ter em consideração a diversidade de populações de interneurónios e suas distintas características, o que nos leva a hipotetizar que diferentes classes de interneurónios estão envolvidas na regulação da transmissão de diferentes aspetos de um estímulo direcionando o processamento de informação para uma ou outra estratégia de codificação. Assim, neste projeto, com o objetivo de esclarecer os mecanismos propostos, eu combinei ferramentas optogenéticas com registos eletrofisiológicos *in vitro* e imagiologia de cálcio com microscopia de excitação de dois fotões *in vivo* para medir atividade neuronal no barrel córtex de ratinho. Combinando expressão de actuadores optogenéticos em células específicas com repórteres optogenéticos, estabeleci um método para dissociar o papel de neurónios inibitórios no processamento sensorial.

Resultados obtidos *in vitro* revelaram um papel distinto na inibição proporcionada por neurónios Stt^+ e PV^+ durante transmissão sináptica de *inputs* talamocorticais. Experiencias *in vivo* suportam os resultados eletrofisiológicos, sugerindo uma relação próxima entre a atividade de interneurónios PV^+ e células excitatórias durante o processamento sensorial. Estes resultados corroboram a minha hipótese inicial de que populações corticais de interneurónios têm papéis distintos na manutenção do balanço entre excitação e inibição durante processamento sensorial. Desta forma, irão guiar futuros estudos no papel das subpopulações de interneurónios nas estratégias de codificação empregues em processamento somatosensorial.

Palavras-chave: barrel córtex, balanço E/I, diversidade de interneurónios, código neuronal, processamento somatossensorial.

Chapter I

Introduction

2.1.1 Sensory coding

Communication between two neurons forms the neural basis of our capacity to perceive sensations from the outside world, to think, to move or to make decisions. Therefore, all the billions of nerve cells that are part of our nervous system are interconnected forming complex neural networks. This neuronal interconnection ensures a correct and tightly regulated long distance propagation of signals.

A nerve cell communicates with others receiving information (input) and retransmitting that information (output), after integration, through functional interactions called synapses. Synaptic transmission occurs through the transmission of discrete and identical electrical transient impulses, known as action potentials or spikes, across a neural circuit in response to a stimulus. In this process, information travels along nerve cells of a neural network through electrically or chemically generated signals. In turn, with the required coding strategies, these signals have the capacity to carry and integrate sensory information to then construct complex thoughts and sensations.

Therefore, in a very summarized definition, the neural code can be characterized as the relationship between an external stimulus and the neuronal response patterns that allows the brain to transmit and interpret its sensory information (Bialek et al., 1991). Additionally, it comprises the mechanisms and rules by which information, perceived from the outside world or intrinsically generated within the neural circuits (Dimitrov and Miller, 2001), is represented by neural activity (Adrian and Zotterman, 1926, Miller, 1994, Shadlen and Newsome, 1994, Brenner et al., 2000, deCharms and Zador, 2000, Stanley, 2013).

As referred above, sensory information is encoded in the brain through complex patterns of action potentials, also known as spike trains (Gerstner et al., 1997). And, although the question of how these spike patterns may represent sensory information in the brain has been being studied for many years, across different systems and through different perspectives, we are still far from establishing general coding principles. Thus, making of the coding strategies underlying the sensory processing and transmission a fundamental unsolved question in the neuroscience field.

1.1.1 Coding strategies

Our understanding of the mechanisms by which information is transmitted from neuron to neuron or by an ensemble of neurons, within a neural network and in order to represent a stimulus, is still far from being clear. Several hypotheses for coding schemes have been proposed. The main difference between them are the properties of a spike pattern used to represent information. This difference is particularly clear between the two currently more strongly supported models: the rate and the temporal code.

1.1.1.1 Rate code

The rate code, also known as frequency code, refers to a coding scheme where information is carried by the firing rate of spikes per unit of time. In other words, the average of times that a neuron fires within a certain interval of time. This coding scheme does not consider the precise timing of each spike and, ideally, the firing timing should be unrelated, being by this reason also known as asynchronous code (Miller, 1994, Kumar et al., 2010). Consequently, should only be applied when there is a strong correlation between the stimuli and the correspondent mean number of spikes in the response and no relevant information would be added by considering the precise firing timing (Theunissen and Miller, 1995).

Therefore, according to a rate coding strategy, the intensity of a certain stimulus should increase proportionally with the number of firing spikes of the related neurons. For instance, the tension or strength of a certain muscle will increase with the firing rate of the motor neurons that innervates (Adrian and Zotterman, 1926, Miller, 1994, Gerstner et al., 1997). This directly proportional correlation was originally demonstrated in 1926 by Adrian and Zotterman with the first sensory fibers electrical activity recordings in muscle cells (Adrian and Zotterman, 1926).

Accordingly, if in several recording trials we obtain variations in the action potential number, in response to the same stimulus, that variation is considered as 'neural noise' by the rate coding scheme (Koyama, 2012). Where, by definition, neural noise is a part of the recorded neural response that may have its origin in random non-stimulus related events and, as result, should not be taken into

consideration (Pouget et al., 2000). For that reason, the rate code should only be applied for single neurons or neuronal populations with long integrative time windows, which allow a higher fidelity in probabilistic terms (Eggermont, 1998).

The rate code was the first solid hypothesis of how information is encoded within the brain circuits, and persisted as the most plausible one for a few decades. However, many authors argued that mean firing rate alone was insufficient to accurately transmit even the simplest stimuli (Gautrais and Thorpe, 1998). They pointed out the processing information speed observed in sensory systems. Then considered the required time for all the inherent processes (such as synaptic activation, spike generation and their transmission through several cortical layers). Considering these two factors, the time left in the time window to integrate signals would be too short for most of the several neurons within the associated circuit, to fire more than one time before those of the next layer have to respond (Thorpe et al., 2001). Consequently, the conventional frequency code would be incompatible with such a fast processing speed. Thus, coding strategies dependent on smaller integration time windows were hypothesized.

1.1.1.2 Temporal code

In 1994, Middlebrooks and colleagues performed a study in the cat auditory system that would be one of the first major indications of the existence of a different coding strategy: the temporal neuronal code. By linking the stimulation of auditory neurons responsible for perceiving the spatial sound location with recorded spike trains, they found a much more accurate correlation in patterns that included information about the spike timing than with conventional spike rates alone (Middlebrooks et al., 1994). Additionally, in a contemporaneous visual object location study, it was found that, by considering only the spike rate counting, a significant amount of information (up to one third) would be lost (Kjaer et al., 1994, Jacobs et al., 2009). These two studies, together with the previous demonstrated limitations of the rate code, led to hypothesize the existence of this different and more complex coding scheme that would take into account the specific firing times – the temporal code.

The temporal coding scheme allows neurons to integrate a higher amount of information in the same spike train (Miller, 1994). This helps to not misread two

similar but distinct neural inputs (Mauk and Buonomano, 2004). Considering, for instance, if in a 10 milliseconds (ms) firing record we obtain 5 APs, according with the rate coding strategy we could only extract this average spike number information. However, from a temporal coding point of view, we could get "0101011100" or "1010011011", within many other spike trains combinations. Being '1' and '0' representations of an action potential or its absence, respectively (Theunissen and Miller, 1995). Therefore, in the temporal code it is not only important to know the precise timing of spikes. Instead, we should also be aware of the interspike intervals – intervals between two action potentials (D'Argembeau et al., 2014). Interspike intervals are particularly important in temporal patterns of tonically active inhibitory neurons. On these cells a pause in action potential firing is translated into a disinhibition signal and, subsequently, in firing of the following neurons (Jaeger, 2007, Steuber et al., 2007). Subsequently, interspike intervals were suggested as having a crucial contribution to excitatory/inhibitory inputs balance (Shadlen and Newsome, 1994, Ostojic, 2011). Combinations of spikes and silence have also been found highly informative when comparing with other coding schemes hypotheses (Schneidman et al., 2011).

In order to facilitate the representation and subsequent interpretation of both, precise timing of the individual action potentials and interspike intervals, a spike train is very often turned into a binary symbols vector, where a spike or its absence (non-spike) are represent with 1 or 0, respectively (Figure 1.1) (Perona, 2014).

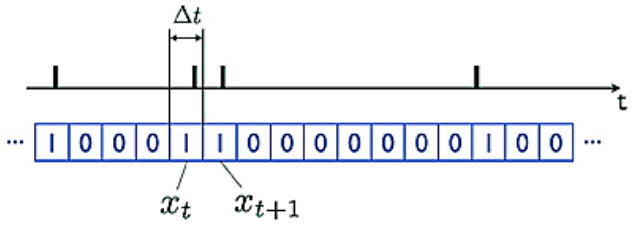

Figure 1.1. Binary representation of a spike train. Reproduced from (Perona, 2014). The individual action potentials produced by a neuron over time (t) are represented with vertical bars. The time window is divided into bins of length Δt. When an action potential is observed, within a bin temporal limit, it is represented as 1 in the corresponding Δt interval and, in contrast, its absence is indicated with 0.

Therefore, a quite good analogy to understand the temporal code complexity and its components is the Morse code. Both allow information transmission and

processing by combining sequences of elements (action potentials or sounds, respectively), their number, intervals, timing and variations (Mauk and Buonomano, 2004).

The temporal code has been widely associated with motor and sensory neural processing. These processes seem to require spatial-temporal patterns with a millisecond scale resolution, considering which sensory neurons are activated during the processing of a certain stimulus. Hence, different sensory stimuli activate distinct neuronal populations, allowing the brain to discriminate between, for instance, a needle skin prick in two different positions. Temporal patterns are also essential to motor information processing due to the required precise temporal synchrony of motor neurons activation to allow correct movement coordination as output. This stimulus processing takes into account the duration of certain sensations and requires the assimilation of the temporal patterns of the spike train (Mauk and Buonomano, 2004). Having said that, most sensory stimuli, such auditory, visual and somatosensory ones, are likely to involve a combination of both spatial and temporal activity patterns for accurate neural processing, underlining the importance of looking into neuronal population coding strategies.

1.1.1.3 Population level: sparse code

In the processing of certain stimuli, which particular neurons are activated is a crucial feature that allow us to discriminate the spatial localization of touch or a sound source (Mauk and Buonomano, 2004). Usually, neuronal cells that are simultaneously activated in response to a specific stimulus, have similar functions, each one being responsible for a set of inputs (D'Argembeau et al., 2014). The firing patterns of these population neurons are then tuned and combined to interpret the input. Therefore, the coded information cannot be accurately extracted from a single nerve cell or by simple summation of individual signals, but by an ensemble of interconnected neurons (Gerstner et al., 1997, Pouget et al., 2000).

Synaptic transmission is highly noisy which means that the exact same pattern of activity rarely occurs twice. Additionally, the representation of information in an ensemble of neurons is highly probabilistic (Averbeck et al., 2006). Thus, coding at a population level should allow a higher temporal and rate resolution, fidelity and

robustness about stimuli features, by reducing possible neuronal firing errors, since more than one neuron is responsible for the transmission of the same signal (Stevens and Zador, 1995). As a result, the consideration of an ensemble of neurons greatly increases the possibilities for other coding schemes or their combination (Theunissen and Miller, 1995).

Regardless of the neuronal information being encoded by the mean rate of spikes or their precise timing, another feature of sensory processing, very strongly supported by several studies in this topic, is the sparse representation of neuronal information. In other words, it has been suggested by a number of studies that sensory information is represented in the brain by the strong activation of a small number of selected neurons, which is reflected into a low activity ratio (Barth and Poulet, 2012). The sparse activity of neuronal populations has been argued as an evolutionary strategy to significantly reduce metabolic energy costs (Graham, 2007). Other authors suggest that sparse code is biologically advantageous to represent and store associative memories by maximizing its capacity (Olshausen and Field, 2004). In fact, this variant of population coding was reported as being particularly useful in the visual system, for instance in face recognition tasks (Wright et al., 2009). Nevertheless, there are also evidences reporting the use of a sparse activation to represent stimuli in other sensory systems, including in the rodents' primary sensory cortex (O'Connor et al., 2010, Barth and Poulet, 2012).

The so far defined parameters for either of the proposed coding strategies above mentioned alone do not seem to be sufficient to clearly understand the processing or representation of sensory information. In fact, one of the current challenges in the field is to try to consensually define or conciliate the principles of the two and integrate them with what we know so far about sensory representations in populations of neurons or neuronal networks.

1.2 Somatosensory processing

The somatosensory system is considered one of the most complex sensory systems. In fact, somatosensory processing embraces the mechanisms that allow us to perceive a number of very different sensations, contributing to our own sense

of self (Nicolelis and Ribeiro, 2006) and including all the neural circuits responsible for touch, temperature, vibration, limb position and pressure.

All these sensations are originated by receptors in different afferent nerve fibers, integrated in skin or muscles, according with the type of sensation: mechanoreceptors – vibration, touch and pressure; proprioceptors – position of body parts; nociceptors – pain and temperature (Lynn, 1975). After activation of these peripheral neuronal receptors, the sensitive information needs to be retransmitted across the whole circuit until it reaches the appropriate cortical neurons, so that complex conscious percepts of external stimuli can be formed. Problems during this processing can lead to a wide range of very debilitating disorders, usually related with behaviour or motor impairment (Cauller, 1995, Metcalfe et al., 2005), social, communication or cognitive disabilities (Porter, 2004, Cascio, 2010). Hence, stressing out the importance of a more clear understanding of how the information is encoded and processed across the somatosensory circuits.

1.2.1 Somatosensory circuits

Between the different animal models used to study mammal sensory processing and somatosensory integration, mice are possibly the most attractive one. Amongst other reasons, as the possibility of using molecular tools combined with the wide range of transgenic mice strains, they share with us a reasonable number of basic brain features (Nicolelis and Ribeiro, 2006, Petersen, 2007). Thus, the rodents' somatosensory system is my elected model to study somatosensory processing in order to help to elucidate the coding principles employed to represent information in the brain. Particularly, the mouse vibrissal somatosensory cortex (vS1) is often chosen for being relatively simple and easy to manipulate.

Rats and mice are nocturnal animals and therefore cannot rely much on visual information. Subsequently, they use whisker movements to collect relevant information from the surrounding environment by sensing slight whisker perturbations when in contact with objects (Diamond et al., 2008, Petersen, 2009). The vibrissal primary somatosensory cortex has been shown to be essential for

simple stimuli detection and discrimination by either passive or active whiskers movement (Miyashita and Feldman, 2013).

Whisker-mediated sensory information allows the animal to perceive sensory signals which can be interpreted to determine a number of features of tactile stimuli, as location, intensity and duration (Nicolelis and Ribeiro, 2006), thus, allowing fine object discrimination (Diamond et al., 2008). Although object features information is more reliable considering signals from multiple whiskers, each whisker by it itself is highly informative (Arabzadeh et al., 2005, Diamond, 2010). Collected tactile information is then used to refine motor control (Figure 1.2-A). For this reason, there are essential interactions between the sensory pathways, particularly from the vS1, and the motor cortex. The last integrates the sensory inputs with motor outputs, leading to an enhanced coordination of whiskers movements, in order to improve tactile sensory perception (Ferezou et al., 2007).

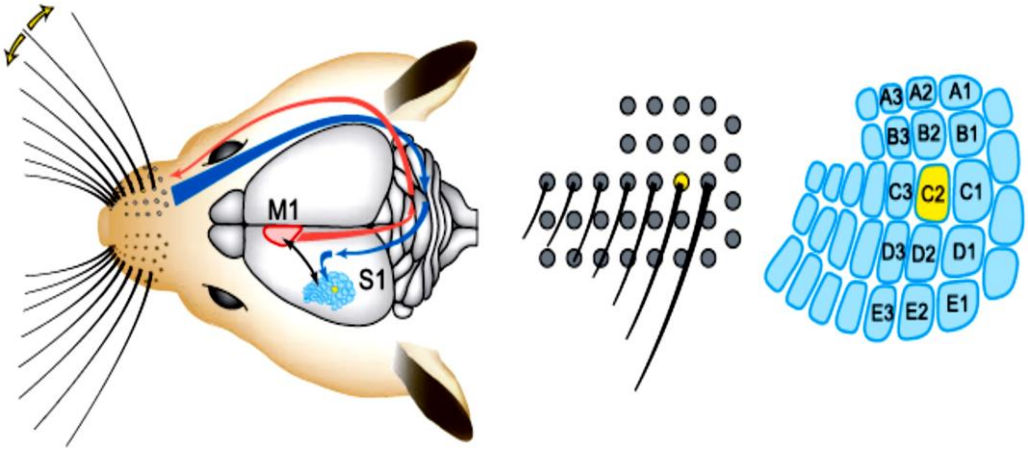

Figure 1.2. Barrel cortex columns-whiskers associative map. Reproduced from (Petersen, 2009). (A) Sensory and motor pathways are represent by blue and red lines, respectively. During active sensory perception, the neuronal signals originated by whiskers' deflection are transmitted by trigeminal nerves until the trigeminal nuclei, in the brain stem. From here, they are transmitted to the thalamic somatosensory nuclei and then to the appropriate barrel in the primary somatosensory cortex. In response, the motor cortex projects information to the brain stem nuclei, which controls whisker motor neurons. **(B)** The layout by which whiskers are organized in the snout is similar with the barrels distribution in the vibrissal primary somatosensory cortex, as exemplified with the whisker and respective barrel highlighted in yellow. **M1** – motor cortex; **S1** – primary somatosensory cortex.

The functional somatotopic columns in which the barrel cortex can be divided are designated barrels and represent different points in the receptive field with the same layout as the whiskers in the snout (Figure 1.2-B) (Diamond et al., 2008, Petersen, 2009, Waxman, 2010). In turn, barrel cortex columns or barrels have a laminar structure and, although more than one column can simultaneously process the same whisker deflection, responses are layer and cell-specific (de Kock et al., 2007). Each of the six cortical layers contains distinct sets of excitatory neurons involved in specific whisker-circuits (Nicolelis and Ribeiro, 2006, Petersen, 2007, O'Connor et al., 2009), allowing delineation of functional organization and plasticity (Petersen, 2007). This organization pattern greatly facilitates the decoding of the stimulated whisker location (Panzeri et al., 2003) and emphasizes how the barrel cortex can be a great model to relate sensory stimuli, specific neuronal responses and subsequent behaviour (O'Connor et al., 2010).

The base of a whisker contains specialized peripheral sensory mechanoreceptors (Nicolelis and Ribeiro, 2006), which convert movements in action potentials patterns through mechanogated ion channels activation (Figure 1.3) (Petersen, 2007, Diamond et al., 2008).

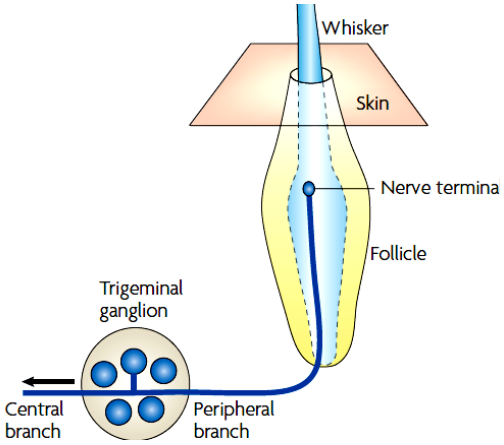

Figure 1.3. Whisker mechanoreceptor terminal. Reproduced from (Diamond et al., 2008). The mechanoreceptors, present at the base of each whisker's follicle, encode information about its deflection and respective direction, velocity and duration. Those sensory fibers carry the information to its cell bodies, located at the trigeminal ganglion, from where it is transmitted to the trigeminal nuclei, in the brain stem.

Whisker-stimulation evoked spike trains are transmitted by the trigeminal nerve to the trigeminal nuclei, which receives vibrissal information from the three parallel pathways: lemniscal, extralemniscal and paralemniscal (Deschênes et al.,

2005) (Figure 1.4). Although the functional differences between these three pathways is still not clear, current knowledge suggests that they are, respectively, responsible for touch (contact and movement); contact timing; movement and object location information (Ghazanfar and Nicolelis, 1997, Veinante et al., 2000, Ahissar et al., 2001, Diamond et al., 2008).

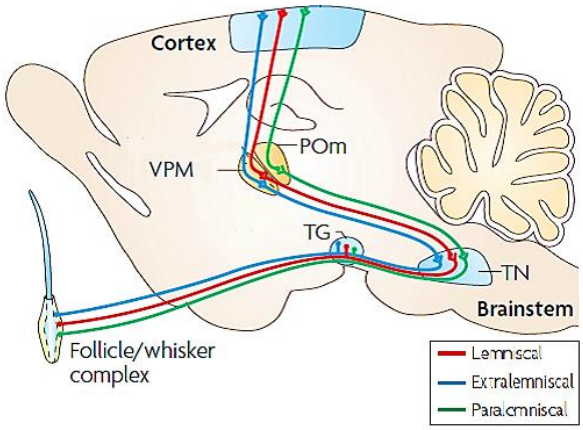

Figure 1.4. Schematic representation of lemniscal, extralemniscal and paralemniscal pathways. Adapted from (Diamond et al., 2008). The sensitive information encoded by the peripheral sensory afferents are transmitted to the trigeminal nuclei (**TN**), in the brain stem, passing through the trigeminal ganglia (**TG**), and, from here transmitted to the thalamic ventral medial posterior nucleus (**VMP**) or to the posterior thalamic nucleus (**POm**), where it is processed before arriving into the somatosensory cortex. This transmission can be carried by three different neuronal pathways: lemniscal, extralemniscal and paralemniscal.

Information from each sensory pathway is processed in a different nucleus of the thalamus. This brain structure is considered a relay station of somatosensory information (Camarillo et al., 2012), subsequently, thalamocortical projections are crucial in outside world sensations perception, by conducting that information to the somatosensory cortex (Bruno and Sakmann, 2006). The lemniscal and extralemniscal signals relays to the ventral medial posterior nucleus of the thalamus (VMP) being the lemniscal information then retransmitted to the primary somatosensory cortex (S1) septa and to the secondary (S2) somatosensory cortex while the extralameniscal information is passed on to the layer 4 of the barrel cortex. The paralemniscal pathway is connected with the posterior thalamic nucleus (POm), that in turn retransmits information to the S1 (layer 5), S2 and motor cortex (M1) (Diamond, 2000).

A great effort has been made to describe and understand the functional organization of the barrel cortex as well as the sensory processing mechanisms within each cortical column. The details of the synaptic transmission dynamics are however still far from being clear. Thus, making of the barrel cortex synaptic connectivity a prominent research object in order to better understand the processing of sensory information.

1.2.2 Coding in the somatosensory system

Since the first experiments with electrical activity recordings in muscle sensory fibers performed in 1926 (Adrian and Zotterman, 1926) it was generally assumed that peripheral afferent neurons primarily encode sensory information by a rate coding strategy. However, many studies since then reported that other coding strategies or a combination of them are used to represent this information, either in the periphery or in upstream pathways (Adrian and Zotterman, 1926, Sejnowski, 1995). Studies in on sensory processing in the rodents' somatosensory system have been corroborating this idea by presenting a number of different principles employed in the encoding of afferent information.

As mentioned before, rhythmic vibrations in the whiskers are converted into signals that allow fine sensory discrimination. This can be improved by combining signals from different whiskers (spatial integration) over several sweeps (temporal integration) (Hipp et al., 2006). Mechanoreceptors associated with these whiskers transmit information to the trigeminal ganglion. Studies have shown that, at this level, tactile stimuli are encoded through differences in response magnitude, in other words, a rate code (Leiser and Moxon, 2007). For instance, a higher velocity whisking stimulus has the capacity to evoke a greater amount of spikes as response (Shoykhet et al., 2000). In contrast, other studies have reported that, at the same level, time-varying stimuli information is represented by specific firing time patterns (Jones et al., 2004, Bale et al., 2015).

Several studies have reported that the thalamus not only retransmits the received tactile information but, depending on the vibrissal afferent pathway, also has the capacity to transform it. Thus, performing different computations in parallel (Ahissar et al., 2000). At the thalamic level, in both, lemniscal and paralemniscal pathways, the magnitude (spike rate) of the response decreases as

the frequency increases. However, while in the VMP the latency remains constant, POm neurons seems to transmit information about whisker-movements frequency by shifts in response latency, which increases with whisking frequency, possibly due to a feedback loop with the vS1. The response latency determines the window available for firing and, subsequently, the spike-count. Hereupon, since the whiskers frequency is, in fact, codified by total spike count and spike timing it is possible that both coding strategies, spike time and spike count, coexist at the thalamic level, (Ahissar et al., 2001).

At a more upstream level, experiments with slowly varying stimuli, such as object location (O'Connor et al., 2013), have shown that a perturbation of a single extra spike in one neuron can induce ~28 extra-spikes in postsynaptic targets, thus profoundly modifying activity patterns. This suggests that, for this type of stimuli features, the barrel cortex uses primarily a rate code, since the average spike count, in large neural populations, is more robust to timing perturbation (London et al., 2010).

In simple rough versus smooth texture discrimination tasks, whisker contacts with the surface lead to a roughness varying-motion signal. This signal is converted in spike trains with the rough texture evoking significantly higher firing rates in barrel cortex than the contact with the smooth one (Connor and Johnson, 1992, von Heimendahl et al., 2007, Ritt et al., 2008, Diamond, 2010). Also, rougher or smoother texture surfaces evoke more or less firing synchrony, respectively. This was found as a more robust code than mean firing rate. Thus, the role of synchronization in texture coding can be established as a complement to firing rate–based codes for large texture differences (Jadhav et al., 2009).

Nevertheless, the temporal pattern of spikes might also contribute to texture discrimination. In discrimination tasks with vibratory rapidly time-varying stimuli, either at trigeminal ganglia or barrel cortex level, the temporal timing patterns allow a better texture discrimination than the rate code alone (Arabzadeh et al., 2006). Spike timing also greatly improves information about spatial location and permits the transmission of significant higher amount of information. Not the pattern timing but the precise timing of the first spike following whisker deflection. Therefore, spike-timing seems to be essential to codify timing varying features of sensory stimuli (Panzeri et al., 2001).

Moreover, in recent studies performed in primates' somatosensory system was observed that fingerprint discrimination of shape and applied force direction was too fast to be possible of being explained by a simple rate code. Additionally, the relative timing of the first spike within a neuronal ensemble, after stimulus onset, could consistently transmit information that would allow that discrimination (Petersen et al., 2002a, b, Johansson and Birznieks, 2004). This suggests that location, shape and texture of an object can be primarily encoded by the relative timing of the first spike (Thorpe and Gautrais, 1997, Thorpe et al., 2001). This would be particularly useful in situations that require a very fast biological response, such as the ones crucial for survival e.g. avoiding a predator (VanRullen et al., 2005). The required reaction time is so short that most of the neurons involved in the process would not have time to fire more than one time (Thorpe and Gautrais, 1997). Then, with a longer encoding time, a rate coding strategy could give more information about stimuli intensity (Johansson and Birznieks, 2004).

Together these studies demonstrate how general principles by which processing of information occurs in the barrel cortex are far from being clear. Although firing rate has been suggested as essential to discriminate between highly distinct features, precise time-spiking was demonstrated as being crucial to distinguish two similar textures or encode information about stimuli with a clear temporal structure (de Kock et al., 2007, Jadhav et al., 2009, O'Connor et al., 2013). This supports the idea that, in order to allow more accurate sensory encoding and perception, rate and temporal coding schemes are very likely to complement each other in a range of possible complex combinations of both strategies. Thus, enforcing the necessity of looking for principles which accept the coexistence of rate and temporal patterns mediated sensory encoding in order to understand sensory processing in the somatosensory system.

1.3 E/I balance on sensory processing

Neurons do not work alone and so neither the different coding strategies can be completely isolated from each other. Whether the information evoked by a certain stimulus is represented by a rate code, the "average number of action potentials per time unit", or by a temporal code, precise timing of individual spikes, remains a

topic of intense debate (Shadlen and Newsome, 1994, Gerstner et al., 1997). Being these two opposite coding schemes and considering how both coding strategies seem to be important to encode information about different stimuli features, an hypothesis of a general coding principles that embrace features of these two distinct coding strategies has been gaining popularity (Kumar et al., 2010).

Amongst other hypotheses, a more general coding strategy, which includes and integrates rate and temporal coding principles as well as synchrony in constant interaction and correlation. Was suggested This hypothesis postulates that neural interactions have a high spatiotemporal dynamics and, thus, they can suffer alterations on synaptic connectivity of a neural population, according with the processing of different synaptic input (Friston, 1997). As a result, it has been argued that temporal code and rate code are not mutually exclusive in stimulus response propagation but are instead the two opposite extremes of a wide range of possible variations (Kumar et al., 2010, Stanley, 2013). Consequently, neural network properties, such as the amount of shared connections and the synaptic couplings' strength, may shift the preference of using a certain neural code amongst others. This is would explain why contradictory studies have been suggesting that an emerging synchrony can either have a negative or positive impact on the propagation fidelity of firing rate (Kumar et al., 2010, Wiggins and Hartley, 2015).

The coding principles that embrace synchrony as an essential feature in sensory processing can be considered as a variant of the temporal code, since they are based in the relative timing of the spikes within a neural network (Friston, 1997). Thus, synchronization of the spike timing of more than one neural population, across different brain areas, would allow a more precise perceptual and cognitive input correlation (Singer, 1999). Still, synchrony greatly affects firing rate through a balance between excitation and inhibition during sensory transmission, Hence, synchronization can occur at a common input level and be of particular importance in regulating the interaction between excitatory and inhibitory synapses during sensory processing (Nowotny et al., 2008).

Synchrony plays an important role in regulating the flow information gate into the cortex. At the cortical level, the temporal coordination of sensory stimuli encoding seems to be particularly important to gate information flow. The precise

timing of firing is determined by fluctuations of synaptic inputs with irregular activity patterns (van Vreeswijk and Sompolinsky, 1996, Cafaro and Rieke, 2010). Subsequently, neuronal populations dynamically adjust so that excitatory and inhibitory inputs are usually synchronously balanced in cortical circuits with a millisecond precision (Wang et al., 2010), where single cells receive finely tuned, detailed balanced excitatory and inhibitory inputs during spontaneous and evoked activity (van Vreeswijk and Sompolinsky, 1996, Okun and Lampl, 2008). This means that, in addition to an overall or global balance, single neurons receive equal amounts of excitation and inhibition. Consequently, at the single cell level, the net membrane current remains zero and action potentials are generally cancelled by default. Thus, in the so called thalamocortical 'gate-off' conditions, the local inhibitory signal needs to be strong enough to cancel random action potential firing (Vogels and Abbott, 2009).

In contrast, in gate-on states, when a prominent alteration in the outside environment occurs, such as a whisker deflection, due to a very precise regulation of spikes, a small change in the input amount over a short time increment generates a relatively large change in the synaptic inputs to the neurons in the network (van Vreeswijk and Sompolinsky, 1996). This leads to a quick adaptation that allows neurons to fire asynchronously, affecting the spike number and timing through a mechanism of thalamocortical feed-forward inhibition that causes a millisecond time scale imbalance (Gabernet et al., 2005). Subsequently, it creates a lag of several milliseconds of inhibition behind excitation disrupting the E/I balance (Okun and Lampl, 2008). As a result, neuronal activity will not be fully cancelled, allowing signal propagation (Pinto et al., 2000, Vogels and Abbott, 2009).

A precise control of synchrony determines the integration window of opportunity to relay information, being influenced by alterations in the normal excitatory/inhibitory balance (Wang et al., 2010), essential to rapid action potentials activation by keeping neurons close to spike threshold (Haider et al., 2013). This ensures that input signals are precisely coordinated and cortical processing is focused on salient stimuli (Wang et al., 2010, Brette, 2012, Stanley, 2013). Therefore, failure in balancing excitation and inhibition in gate off states can lead to neurological conditions in which an incomplete gating off of signals

may be a possible cause for an impairment in discrimination between external an internal stimuli (Vogels and Abbott, 2009). Furthermore, while excessive inhibition prevents neuronal activity propagation, abnormally increased excitation leads to seizures (Moore et al., 2010). Accordingly, an impairment in E/I balance during somatosensory processing has been strongly associated with abnormal sensory processing in a number of neurological diseases (Rubenstein and Merzenich, 2003, Lewis et al., 2005, Yizhar et al., 2011, Zhang Z., 2011).

Neurons operate as coincidence detectors controlling the time window for integration of excitation (Okun and Lampl, 2008). In fact, in a recent study, using optogenetic tools, patterns of neural activity were recorded and shown sufficient to obtain a certain behavioural response, when mimicking their natural activity. Then, it was observed that when changing the precise spike timing patterns, by inducing an impairment in excitatory/inhibitory balance of specific cells of the circuit, the firing synchrony was lost and also the correct behavioural response (O'Connor et al., 2013). These results stress the importance of precise spike timing to process certain types of information and an adequate excitatory/inhibitory synaptic balance to maintain that timing (Hausser and Smith, 2007, Packer et al., 2013).

Therefore, precise asynchronous spike timing can be an essential feature for neurons in order to have specific action potential patterns, enabling information transmission (Vogels et al., 2011). In other words, according to this hypothesis, information is permitted to be transmitted from the thalamus to the cortex when excitatory and inhibitory inputs are differently modulated or a faster excitatory signal transiently overcomes inhibition (Vogels and Abbott, 2009). An evoked-activity dependent alteration in action potentials rise time, which in turn induce gain modulation activation in upstream circuits, has been suggested as a possible mechanism for this change in E/I balance (Moore and Nelson, 1998). In turn, these alterations can possibly be regulated through differential cholinergic inputs modulation from the brain stem or by inhibitory synapses plasticity (Vogels and Abbott, 2009, Poulet et al., 2012).

1.3.1 Role of inhibition

Together with the increasingly number of evidences supporting the importance of the role of the balance between excitation and inhibition in sensory processing, have been emerging the hypothesis that activity of specific neuronal populations differently regulate and shape the perceived information of salient stimuli rather than just an overall balance between excitation and inhibition (Vogels et al., 2011). This assumption is in accordance with the suggested sparse cortical activity observed so far in stimuli processing of several sensory systems (Mateo et al., 2011, Avermann et al., 2012, Haider et al., 2013). In other words, during integration of sensory stimuli at the cortical level, only a small population is usually responsive.

Event thought inhibitory GABAergic neurons represent only a small percentage, ~15%, of the cortical neuronal population they have a very dense connectivity in the cortex, being connected to all local excitatory pyramidal cells of the respective microcircuit (Fino and Yuste, 2011, Packer and Yuste, 2011, Avermann et al., 2012). As cortical inhibitory neurons usually receive more excitatory inputs than excitatory nerve cells (Mateo et al., 2011, Haider et al., 2013), inhibition governs activity in the cortex by default. Thus, cortical processing is driven into a sparse code by activation of only a subset of neurons when the excitatory/inhibitory balance is disrupted, allowing a precise and stimulus-specific time window of opportunity for sensory integration (Wilent and Contreras, 2005, Barth and Poulet, 2012). Therefore, fluctuations in inhibitory synapses need occur in order to cancel correspondent variations in excitatory synaptic inputs, which leads to a strong correlation between the two. As a result, during the so called 'gate off' states, the larger the excitatory signal in the local circuit, the larger the inhibitory one will be (Cafaro and Rieke, 2010).

Several studies in different sensory systems reported inhibitory circuit's plasticity as a possible mechanism to sharpen receptive fields by filtering relevant information and supressing activity of non-responsive neurons (Foeller et al., 2005, Galindo-Leon et al., 2009, Sohal et al., 2009, Lee et al., 2012). A good example of this mechanism is a study involving the measurement of activity in neuronal populations of the female mice auditory cortex responsive to calls of lost pups.

When comparing between virgins and mothers, was observed that the overall neuronal population activity was actually smaller in mothers, even though they had significantly better stimuli-responses. Instead of increasing the activity of stimuli related neurons, it had occurred an overall reduced of activity promoted by inhibitory plasticity in non-responsive ones. Thus, as the excitatory responses are more prominent within the relevant microcircuit, there is an enhancement in signal-to-noise ratio, sharpening the receptive field and improving behavioural responses (Galindo-Leon et al., 2009).

Moreover, subtle changes in inhibition strength can lead to the emergence of long-latency suprathreshold responses to stimulation (Moore and Nelson, 1998). As a matter of fact, in cortical synapses with correlated activity, activity-evoked E/I unbalance through potentiation of excitatory synapse is recovered with a compensatory increase in inhibition through plasticity mechanisms when the stimulus is no longer a novelty or is actively being presented (Vogels et al., 2011).

Thus, inhibition is involved in the regulation of the balance between excitatory and inhibitory activity through different possible mechanisms. Either by increasing or decreasing inhibitory activity in coordination with excitation, inhibition seems to have a critical role in gating the flow of information to the cortex.

1.3.1.1 Interneurons populations diversity

When looking at sensory processing, it is important to consider the diversity of neuronal populations on the cortex and their putative role during synaptic transmission in the respective circuit. Such cellular diversity might have a key role when combining coding strategies or shifting towards one of them during sensory processing and according the specificities of the stimulus (Chabrol et al., 2015).

Inhibition in the cortex is ruled by different types of γ-aminobutyric acid (GABA) expressing inhibitory neurons which greatly vary in their morphological and physiological properties, amongst others: spine density, channel composition, connectivity, axonal and dendritic branching patterns and neuropeptide content (Ascoli et al., 2008, Moore et al., 2010). Two well-described types of inhibitory neurons which have been associated with inhibition balancing during sensory processing are the parvalbumin (PV^+) and the somatostatin (Stt^+) expressing ones. As they are sensitive to diverse types of sensory inputs, the two types of

interneurons might have roles in coding processes responsible for the transmission of different types of stimuli (Moore et al., 2010). As a matter of fact, in a recent study in which activity of different interneurons was measured through calcium-imaging of genetically defined cells in a awake behaving mice, was demonstrated that different interneurons subtypes encode different features of the same stimuli during discrimination tasks (Pinto and Dan, 2015).

Parvalbumin-expressing interneurons are highly sensitive, exhibiting strong, fast and reliable activation even with weak sensory inputs (Moore et al., 2010, Pala and Petersen, 2015). Additionally, this interneuron subtype provides broad inhibitory output to excitatory local cells and establishes synapses with the soma of the target neurons (Avermann et al., 2012, Estebanez et al., 2015). This leads to a precise regulation of the window of opportunity for sensory integration, as these neurons are capable of creating brief imbalances between excitation and inhibition. Thus allowing spiking and signal transmission during the periods in which excitation dominates over inhibition (Moore et al., 2010).

In contrast, somatostatin-expressing interneurons have a more temporally dispersed regulation as, in addition, to the necessity of a more sustained stimulation, they require sustained facilitating pre-synaptic spiking or a larger number of synchronous pre-synaptic inputs (Pala and Petersen, 2015). On other hand, this type of interneurons is often described as regular spiking adapting neurons as they present a strong short-term facilitation and their spiking rate is closely regulated with the activity of local excitatory neurons (Pala and Petersen, 2015, Trachtenberg, 2015). Stt^{+} interneurons establish synapses with the distal dendrites of the target cells and have been reported as having a disinhibition effect on nearby excitatory neurons by targeting local inhibitory neurons of different subtypes (Cottam et al., 2013, Xu et al., 2013, Estebanez et al., 2015, Sturgill and Isaacson, 2015).

1.6 Objectives

Considering their distinct characteristics, inhibitory neurons subtypes might regulate sensory processing by influencing the properties of the sensory coding strategies employed. PV^+ neurons are more likely to be essential in mechanisms that regulate temporal coordination during sensory encoding due to their fast-spiking properties, crucial for a strict regulation of the temporal window of opportunity for sensory integration. On other hand, Stt^+ inhibitory neurons require a sustained inhibition and have a slower longer-lasting activation with less fine temporal regulation. Taking into account these characteristics, PV^+ and Stt^+ neurons are likely to distinctly contribute to the maintenance of a balance between excitation and inhibition, thus shifting processing of information towards a temporal or a rate coding strategy, respectively.

Therefore, in this project, aiming for a better understanding of the coding strategies employed in somatosensory processing, I propose to test the hypothesis that two classes of interneurons, PV^+ and Stt^+, differently affect the processing of somatosensory stimuli in the mouse barrel cortex. Therefore, the main objectives in this project are:

1) **Establishing an optogenetic approach for cell-type specific activity manipulation and recording of neural activity**

   The success of this project requires the selective manipulation of activity of the two inhibitory neurons and monitoring its effect on other cells or neuronal populations. I will establish an optogenetic approach that allow me to very precisely control and monitor neural activity with high temporal resolution. To achieve this I will combine cell-type specific expression of optogenetic actuators and reporters with the appropriate transgenic mouse strains.

2) **Study the role of inhibition in thalamocortical synaptic transmission *in vitro***

   Different interneurons subpopulations are likely to have distinct roles on synaptic transmission during sensory processing. One of my objectives is to validate this hypothesis on somatosensory system circuits. Thus, I will dissociate the role of Stt^+ and PV^+ inhibition on synaptic transmission of

thalamocortical inputs, by selectively manipulating the activity of the two interneurons. I will record the effect of this inhibition in excitatory neurons in layers 4 and 2/3 of the somatosensory cortex. I will achieve this by combining whole-cell patch clamp electrophysiological recordings with optogenetic photostimulation in mice brain slices.

3) **Evaluate the effect of altered E/I balance in somatosensory processing *in vivo***

   A balance between excitation and inhibition has been strongly suggested as essential for an adequate processing of sensory information. The role of inhibition has been of particular interest. In this project, I aim to assess the effect of altered activity of particular interneurons subpopulations in somatosensory processing. I will manipulate the activity of specific inhibitory neurons populations with an optogenetic actuator. I will record its effect on the neuronal network using non cell-specific optogenetic reporters during whisker-mediated sensory stimulation.

Figure 2.1 illustrates the overall methodological approach to achieve the objectives here proposed.

Chapter II

Materials and Methods

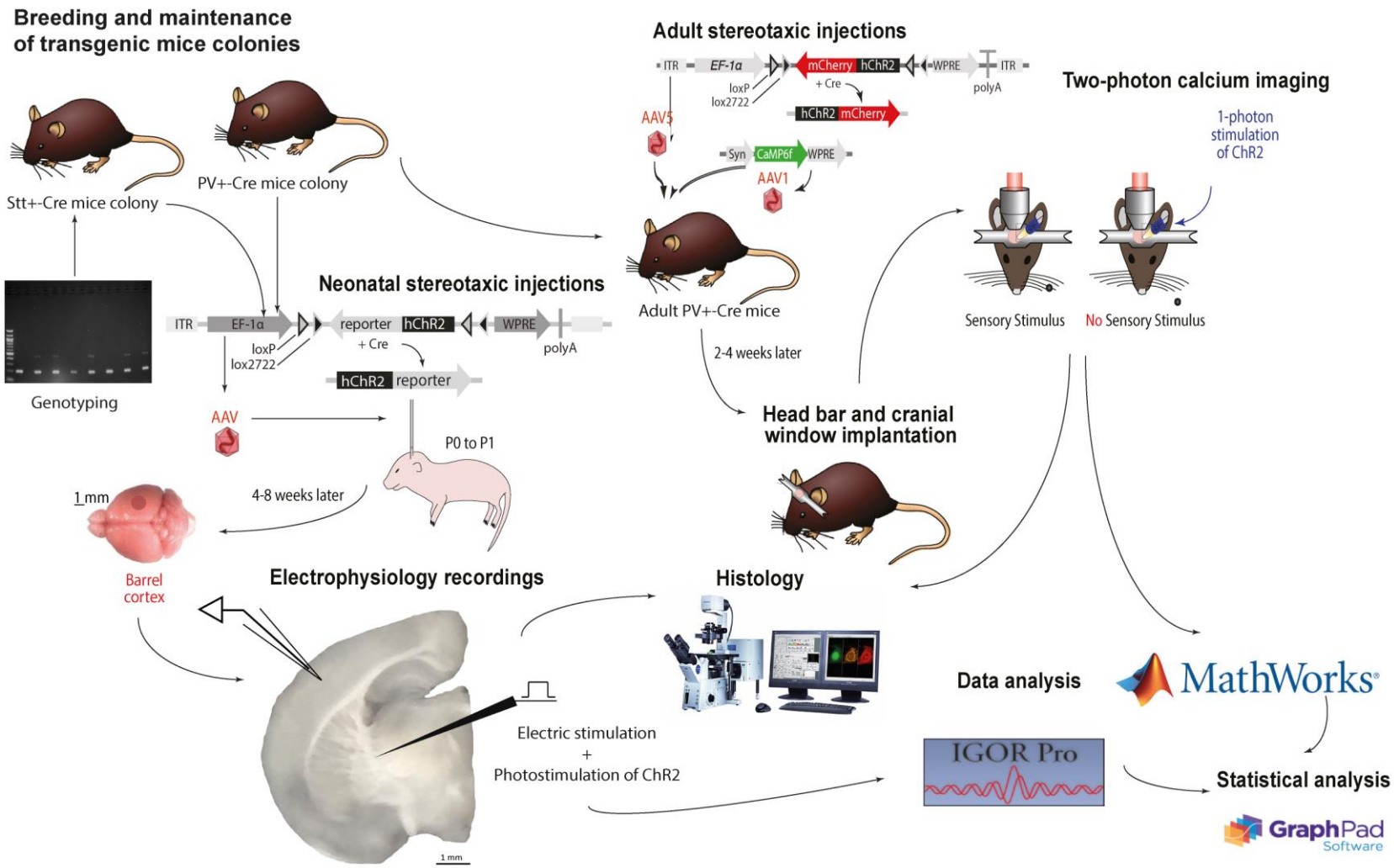

Figure 2.1. General materials and methods scheme.

2.1 Breeding and maintenance of transgenic mice

Cohorts of homozygous PV^{+}-Cre or Stt^{+}-Cre mice were kept in continuous breeding. Mice were weaned at postnatal day (P) 21 and then housed in groups of 4-6 mice from the same sex and litter in individually ventilated polycarbonate cages with food and water *ad libitum*. The housing room was maintained at room temperature of 23 ± 1^{o}C, humidity of 40 ± 10% and on 12 h light/dark cycles beginning at 7 a.m., with lights during the day. All animal experimental procedures were approved and carried out in accordance with the British Home Office regulations.

2.1.1 PV^{+}-Cre transgenic mice

B6.129P2-Pvalb$^{tm1\ (cre)\ Arbr}$/J (stock 017320 from The Jackson Laboratory) or PV^{+}-Cre is a transgenic strain of C57BL/6J mice. PV^{+}-Cre knock-in mice express the Cre recombinase enzyme in parvalbumin-expressing interneurons (IN), without disrupting endogenous parvalbumin (PV) expression. Animals used were breed from a homozygous colony from one of our collaborators in the university (Dr Dennis Kaetzel, Department of Experimental Psychology, University of Oxford, UK).

2.1.2 Stt^{+}-Cre transgenic mice

STOCK Sst$^{tm2.1\ (cre)\ Zjh}$/J (stock 013044 from The Jackson Laboratory) or Stt^{+}-Cre is a transgenic strain of B6129SF1/J mice. Stt^{+}-Cre knock-in mice express the Cre recombinase enzyme in somatostatin-expressing INs, without disrupting endogenous somatostatin (Stt) expression. A homozygous colony of Stt^{+}-Cre mice was established after mating genotyping-positive homozygous (Stt$^{+\text{-}Cre}$ / Stt$^{+\text{-}Cre}$), selected from a F1 litter obtained by crossing a pair of heterozygous (Stt$^{+\text{-}Cre}$ / Stt^{-} ^{WT}) transgenic breeders, recently acquired by another of our collaborators in the university (Professor Colin Akerman, Department of Pharmacology, University of Oxford, UK).

2.1.2.1 Genotyping

Ear clips were obtained from young (< 3 weeks) mice to identify transgenic homozygous or heterozygous mice. A 200 µl volume of lysis buffer (50 mM Tris-HCl pH 8.0, 50 mM EDTA pH 8.0, 0.5% Tween-20) and 2 µl of proteinase K (20 mg/ml; Sigma-Aldrich) was added to each ear clipped tissue in individual

microcentrifuge tubes and incubated for 4 h at 37°C. The digested tissue was heated at 100 °C for 10 min and centrifuged for 1 min. 2 µl of the supernatant were taken as the template for a 20 µl polymerase chain reaction (PCR) mixture in the presence of 10 µl of Ready Mix Taq PCR Reaction Mix (Sigma-Aldrich) and 1 µl of deionized water (ddH_2O). To each PCR reaction tube it was added 1 µl of each wild type and Stt$^+$-Cre mice specific primers: reverse (GGG CCA GGA GTT AAG GAA GA), wild type forward (TCT GAA AGA CTT GCG TTT GG), mutant forward (TGG TTT GTC CAA ACT CAT CAA). After running the PCR program (Table 2.1.), 5 µl of 100 bp DNA ladder (New England, Biolabs) and 5 µl of each one of the amplified DNA samples were loaded into a 1.5% agarose gel with Ethidium Bromide. To avoid DNA sample cross contamination, samples were loaded in adjacent wells. The electrophoresis was run for 30 min at 120 mV and the gel visualized in a Gel Doc XR+ System (Bio-Rad) transiluminator (Figure 2.2).

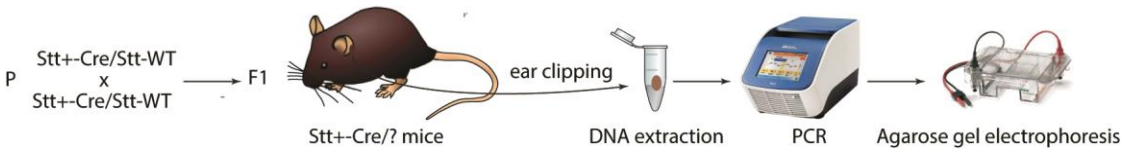

Figure 2.2. Genotyping method simplified scheme. Ear clipping was performed in a F1 litter of 8 transgenic Stt+-Cre mice obtained per crossing of a heterozygous breeding pair. DNA was then extracted from tissue samples and amplified through PCR. **F1** – first filial generation; **P** – parental generation; **PCR** – Polymerase chain reaction.

Table 2.1. Genotyping PCR program. Listed is the temperature and duration used in in each step of the polymerase chain reaction used to amplify sample tissues DNA for genotyping, as well as the respective number of cycles.

Step	Temperature (°C)	Duration	
Initial denaturation	94	2 min 21 s	
Denaturation	94	30 s	**35x**
Annealing	56	30 s	
Elongation	72	30 s	
Final elongation	72	7 min	
Hold	4	∞	

2.2 Viral intracerebral microinjections

In order to obtain brain slices for electrophysiological recordings with optogenetic stimulation neonatal PV$^+$-Cre and Stt$^+$-Cre transgenic mice were injected with chanelrhodopsin 2 (ChR2). For calcium-imaging experiments combined with photostimulation, weaned or adult PV$^+$-Cre transgenic mice were injected with ChR2 and with the genetically encoded calcium-imaging indicator GCaMP6f.

2.2.1 Neonatal mice stereotaxic injections

P0 to P1 PV$^+$-Cre or Stt$^+$-Cre mice were hypothermia-induced anesthetized by being kept in wet paper tissue in a container with crushed ice for about 5 min. Neonates were then placed in a custom-made clay stage and fixed with paper tape on the neck. rAAV5/EF1α-DIO-hChR2(H123A)-mCherry-WPRE (6x10e12 vg/ml) (Figure 2.3-A) or rAAV2/EF1a-DIO-hChR2(H134R)-eYFP-WPRE (3.9x10e12 vg/ml) virus (Figure 2.3-B; for vectors outline and sequences see http://www.optogenetics.org), both purchased from the University of North Carolina Vector Core, were microinjected through micropipettes with ~10 µm Ø pulled from thin-walled borosilicate glass capillaries (outer Ø: 1.14 mm, inner Ø: 0.53 mm; Drummond Scientific) using a horizontal micropipette puller (P-97 Sutter Instruments) via an automated injector (Nanoject II, Drummond Scientific) unilaterally, in three distinct sites above the right barrel cortex (from lambda: anteroposterior (AP) = -1000 µm, mediolateral (ML) 1450 µm; AP = -1000 µm, ML = 1750 µm; AP= -1300 µm, ML = 1600 µm) at four depths (800, 600, 400 and 200 µm below the pia surface), 23 nl per injection site.

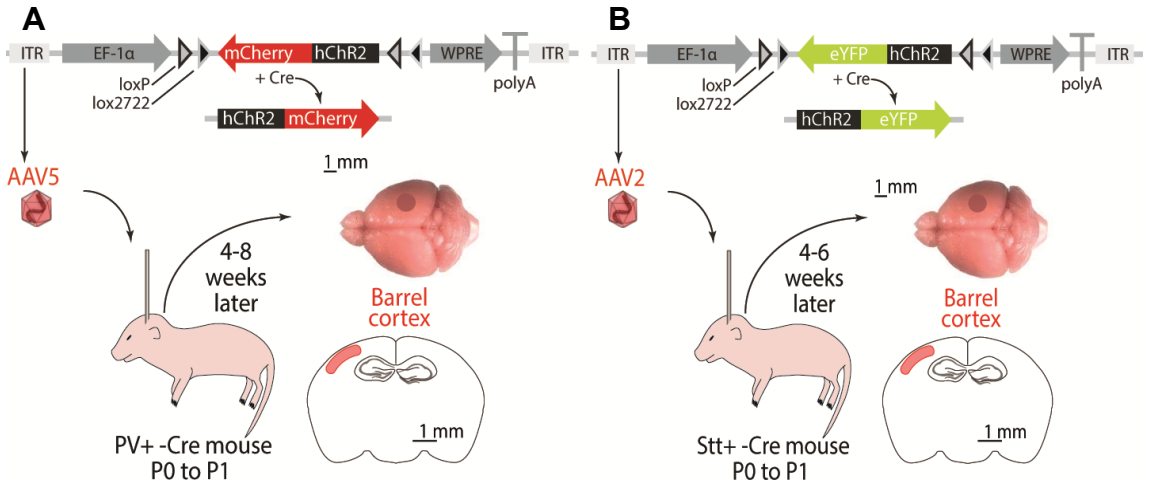

Figure 2.3. Neonatal stereotaxic injections virus constructs simplified scheme. PV⁺-Cre **(A)** and Stt⁺-Cre **(B)** animals were injected with a double-floxed inverted (**DIO**) humanized version of channelrodopsin2 (**hChR2**) coupled to mCherry or yellow fluorescent protein (**eYFP**), respectively, in the right hemisphere of the barrel cortex. Brains from injected animals were used in further experiments after allowing enough time for virus expression. **AAV** – adenoassociated virus; **EF1α** - elongation factor 1α; **ITR** - internal ribosome entry site; **P**-postnatal day; **WPRE** - woodchuck hepatitis virus posttranscriptional regulatory element.

2.2.2 Adult mice stereotaxic injections

2 days before surgeries, adult PV⁺-Cre mice were habituated to plain jelly consumption. For surgeries, mice were anesthetized by inhalation of isoflurane 2–4% at 0.6 –1.4 L/min and placed in a stereotaxic frame. During surgeries, mice were kept in an adequate anaesthesia level through continuous inhalation of isoflurane. Level of anaesthesia was confirmed by cessation of pain reflexes (tested by paw withdrawal to firm fingernail pinch). After local pre-treatment with the anaesthetic marcain (2 mg/kg), the skin on top of the head was retracted. A hole was then drilled in the skull, unilaterally, above the right barrel cortex (anteroposterior = 1300 µm, mediolateral 2900 µm from bregma). An 1:1 mix of rAAV5/EF1α-DIO-hChR2(H123A)-mCherry-WPRE virus (6x10e12 vg/ml) (for vector outline and sequence see http://www.optogenetics.org) with the virus AAV1/Syn-GCaMP6f-WPRE-SV40 (6.91x10e13 vg/ml) (Figure 2.4), both purchased from the University of North Carolina Vector Core, were microinjected through micropipettes with ~10 µm Ø pulled from thin-walled borosilicate glass capillaries (outer Ø: 1.14 mm, inner Ø: 0.53 mm; Drummond Scientific) using a horizontal micropipette puller (P-97 Sutter Instruments) via an automated injector

(Nanoject II, Drummond Scientific) at four depths (800, 600, 400 and 200 µm below the pia surface), 3 times 23 nl per injection site. Micropipettes were left in place an additional 5 min after each bolus injection to ensure diffusion of vector. Micropipettes were then slowly retracted, the scalpel incision closed with sutures and tissue glue. After surgeries, mice were subcutaneously treated with analgesics (metacam, 5 mg/kg and vetergesic, 0.08 mg/kg). As post-surgical care, mice that undergo into surgeries were housed together and supplied with jelly mixed with low doses of analgesics (metacam and vetergesic) for 24 to 72 h, to aid recovery.

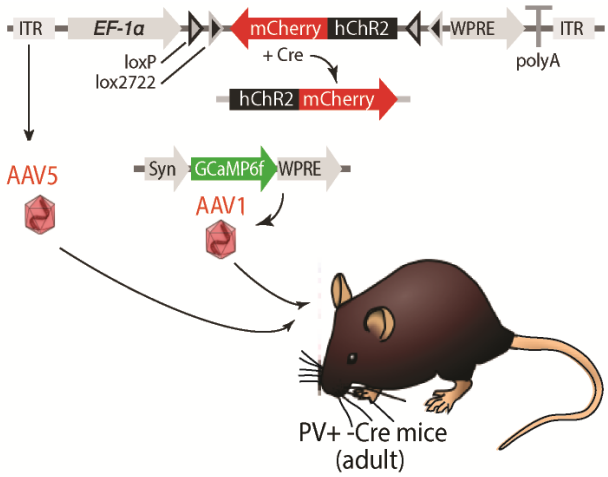

Figure 2.4. Adult stereotaxic injections virus constructs simplified scheme. PV⁺-Cre adult mice were injected with a double-floxed inverted (**DIO**) humanized version of channelrodopsin2 (**hChR2**) coupled to mCherry and the fast version 6 of the genetically encoded calcium indicator GCaMP (**GCaMP6f**) in the right hemisphere of the barrel cortex. **AAV** – adenoassociated virus; **EF1α** - elongation factor 1α; **ITR** - internal ribosome entry site; **Syn –** synapsin promotor; **WPRE** - woodchuck hepatitis virus posttranscriptional regulatory element.

2.3 Electrophysiology

2.3.1 Acute brain slices preparation

4 to 8 weeks old PV⁺-Cre mice of sexes injected with floxed humanized Chanelrhodopsin 2 (hChR2) (AAV5/EF1a-DIO-hChR2(E123A)-mCherry-WPRE) and 4 to 6 weeks old Stt⁺-Cre mice of both sexes injected with floxed humanized ChR2 (rAAV2/EF1a-DIO-hChR2(H134R)-eYFP-WPRE) (Figure 2.3) were deeply anaesthetized by inhalation of isoflurane 4-5% at 2 L/min. Upon cessation of pain reflexes, tested by paw withdrawal to firm fingernail pinch, the animals were decapitated, in accordance with the British Home Office regulations.

The bones and dura mater covering the cortical surface were carefully peeled away and the brain was swiftly removed in ice-cold (0 to 4 ^{o}C) artificial cerebrospinal fluid (aCSF) (Table 2.2). aCSF was bubbled with carbogen gas (95% O_2 and 5% CO_2) for at least 30 minutes before use. The brain was placed on a 10 ^{o} cutting template ramp with the anterior end downhill, as described by Agmon and Connors (Agmon and Connors, 1991).

Table 2.2. Composition of the artificial cerebrospinal fluid. Listed is the concentration of each compound used in making artificial cerebrospinal fluid as well as the final pH and osmolarity.

Compound	Final concentration (mM)
Calcium chloride	2
Glucose	10
Magnesium sulphate	2
Monosodium phosphate	1.25
Potassium chloride	3
Sodium bicarbonate	24
Sodium chloride	126
pH	7.2-7.4
Osmolarity	285 to 300 mOsm 1^{-1}

The sectioned ventral part of the hemisphere was glued to a vibratome plate using cyanoacrylate adhesive. Thalamocortical slices (350 μm) were cut with a semi-automated vibratome (VT1200S, Leica) in cold aCSF. Slices in which the hippocampus was visible and the cortex midline had a 90 ^{o} angle appearance were selected for recordings (Figure 2.5).

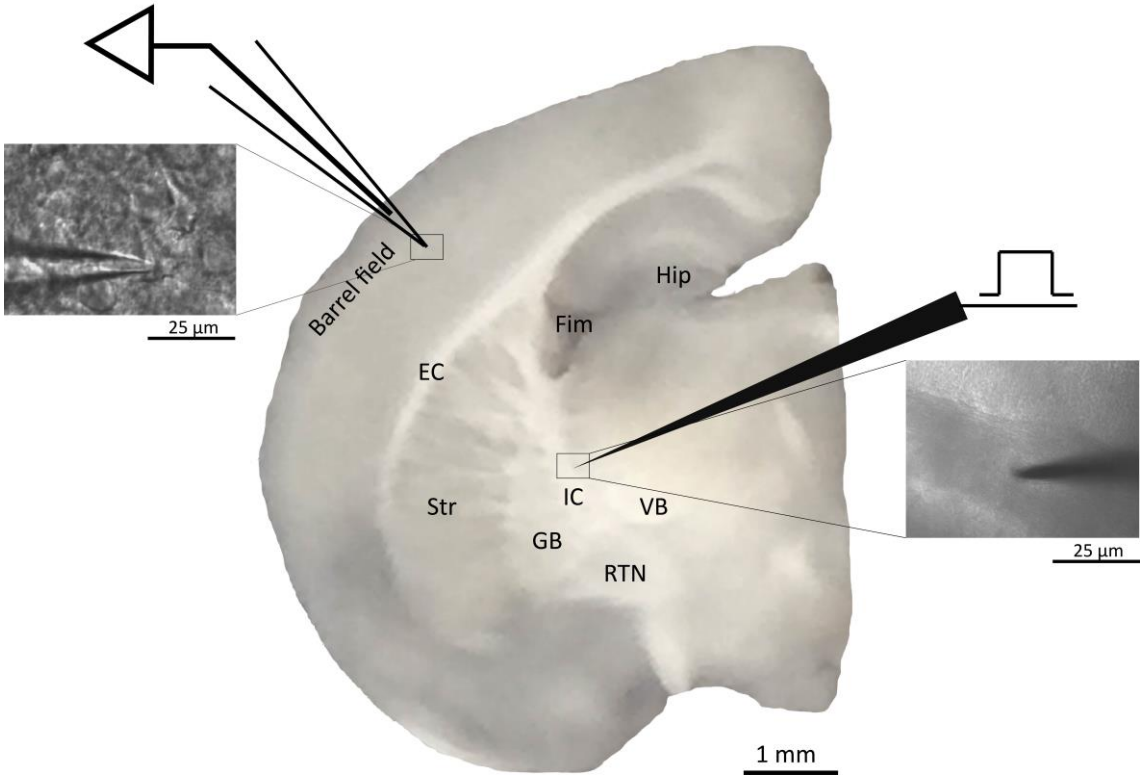

Figure 2.5. Typical slice selected for recordings and typical position of the recording and stimulating microelectrodes marked on an unstained living image of a thalamocortical slice. Dorsal is up, medial is right. **EC**, external capsule; **Fim**, fimbria; **GP**, globus pallidus; **Hip**, hippocampus; **IC**, internal capsule; **RTN**, reticular thalamic nucleus; **Str**, striatum; **VB**, ventrobasal nucleus.

2.3.2 Electrophysiology recordings

Slices were incubated in the dark, at room temperature (20 to 25 ^{o}C), for at least one hour to recover neural network functionality. For recordings, slices were transferred to a submerged-type recording chamber and superfused with aCSF at room temperature, bubbled with carbogen gas, at a high flow rate (3 to 5 ml/min). Whole-cell recordings pipettes with tip resistances of 3 to 8 MΩ were pulled from standard-wall borosilicate glass capillaries (outer Ø: 1.5 mm, inner Ø: 0.86 mm; GC150F-10, Harvard Apparatus) using a horizontal micropipette puller (P-97 Sutter Instruments). Measured voltages were not corrected for the liquid–liquid junction potential of -15.5 mV, calculated using the built-in function of pCLAMP (Axon Instruments).

Cells were visualized using an upright microscope (SOM, Sutter Instruments) with a 40x water-immersion lens equipped with infrared differential interference contrast optics and epifluorescence illumination. Putative cells in layer 2/3 or layer 4 of the barrel cortex (Figure 2.5) were selected for recordings.

All cells from which recordings were obtained were tested for spiking patterns to injection of current steps from -200 pA to 200 pA with a duration of 300 ms and without blue light (470 nm) stimuli pulses coordinated with the injection of current.

Neurons were filled with biocytin during recordings and processed for post-histological identity confirmation.

2.3.2.1 Current-clamp

Whole-cell current-clamp recordings were made with pipettes filled with potassium gluconate-based intracellular solution (Table 2.3). The amplifier was in bridge mode. Capacitance compensation was maximal and bridge balance (9 to 16 MΩ) was regularly adjusted during the recordings.

Table 2.3. Composition of current clamp intracellular solution. Listed is the concentration of each compound used in making intracellular solution for current-clamp as well as the final pH and osmolarity. Final pH was adjusted with caesium hydroxide and potassium hydroxide.

Compound	Final concentration (mM)
ATP-magnesium salt	4
GTP	0.3
HEPES	40
Potassium gluconate	110
Sodium chloride	4
pH	7.2-7.4
Osmolarity	280 to 300 mOsm 1^{-1}

2.3.2.2 Electric and optogenetic stimulation

After a whole-cell recording configuration was established the membrane voltage was kept at < -65 mV for current-clamp recordings. Then, electrical stimulation was applied in the internal capsule (IC) using an extracellular stainless steel

electrode connected to an isolated stimulator (DS3, Digitimer) (Figure 2.5). The stimulation amplitude and duration was set when a stimulus of 15 x 5 mV x 2 ms was able to produce stables excitatory post-synaptic potentials (EPSPs), or action potentials when EPSPs were not detectable, in about 50% of the stimuli (20 to 300 μA in layer 4 and 3 to 11 mA in layer 2/3). Thalamocortical stimulation responses were recorded using ten electric stimulation protocols with 5 different frequencies (2, 5, 10, 20 and 30 Hz) repeated twice in a randomized order and with different time intervals in between. During the electric stimulation protocols, pulsed blue light (470 nm) stimuli were delivered through the epifluorescence pathway of the microscope using a LED light simultaneously with the electric stimulation. All recordings were also performed without photostimulation.

2.3.3 Data acquisition

Data was acquired at 5 kHz and low-pass filtered at 2 kHz with an Axon Multiclamp 700B amplifier (Molecular Devices). The signal was recorded on a computer using the whole cell analysis electrophysiology WinWCP acquisition software (Strathclyde).

2.3.4 Histology and immunohistochemistry

After electrophysiological recordings, brain slices recovered in the dark at room temperature (20 to 25 ^{o}C) for 15 min after the last recording and were then transferred to 4% paraformaldehyde solution (PFA). After overnight incubation at 4 ^{o}C in PFA, slices were washed 3 times in 0.1 M phosphate buffered saline (PBS) solution and stored in the same solution at 4^{o}C until being used for staining. . Brain sections were treated with 0.1% 100X Triton and blocked in 20% normal donkey serum for 1 hour followed by 4^{o}C overnight incubation in primary antibodies diluted in 5% normal donkey serum (Sigma-Aldrich).

To label PV^{+} neurons, it was used the primary antibody guinea-pig anti-PV (1:1000, polyclonal, SYnaptic SYstems) followed by a secondary anti-guinea pig antibody coupled to aminomethylcoumarin (AMCA) (donkey, 1:250, polyclonal, Jackson ImmunoResearch).

Stt$^+$ neurons were labelled using primary rat anti-Stt (1:400; Merck Millipore) followed by secondary polyclonal donkey anti-rat Alexa Fluor 488 (1:1000; Life Technologies).

Primary antibody against mCherry (rat anti-mRP, 1:200, monoclonal, ChromoTek) followed by a secondary anti-rat antibody coupled to Cy3 (donkey, 1:200, polyclonal, Jackson ImmunoResearch) were used to enhance the mCherry signal of PV$^+$-Cre neurons infected with ChR2-mCherry. In the case of Stt+ neurons, ChR2-eYFP expression was assessed with mouse anti-GFP (1:200; Invitrogen), enhanced with polyclonal donkey anti-mouse 568 (1:1000; Life Technologies).

Streptavidin coupled to Texas Red Avidin D (1:1000, Invitrogen), amplified with Biotinylated anti-avidin (1:100) was used to reveal biocytin filling of neurons from which electrophysiological recordings were obtained.

Images of this last staining were obtained with an epifluorescence microscope (DMRB, Leica) equipped with an oil-immersion 40x/0.8 NA objective. All other images were obtained using a laser scanning confocal microscope (FV1000, Olympus) equipped with an air 20x/0.75 NA and an oil-immersion 40x/0.8 NA objective.

2.3.5 Data analysis

All data analysis was performed using custom-written procedures in Igor Pro (Wavemetrics).

Electrophysiological properties of cells were obtained offline by measuring the following parameters obtained by steps of current injection, immediately after establishing whole cell configuration. Input resistance was calculated as the difference in the corrected mean Vm in the first current injection divided by the amount of current injected. Action potential (AP) Vm amplitude was measured as the difference from threshold to peak in the first AP, and AP half-width was calculated as the full width of the AP at half of its maximum amplitude measured from threshold to peak. Rheobase was defined as the smallest current amplitude in the current-step protocol able to evoke a single action potential. Interspike interval adaptation was computed as the difference between the interspike interval of between the two last APs and the two first AP in the current step with higher maximum spike frequency. Maximum firing frequency (Hz) was calculated taking

into account the highest number of AP evoked during current injections and considering the period of time of the respective current step. Resting membrane potential (Vm).

Cells that required a current injection higher than -200 pA to keep mV <-65mV during current-clamp recordings were rejected for electric stimulation recordings. From these, only recordings in which baseline drift was <5% and with ~50% response rate to stimulation were selected for analysis. Effect on synaptic transmission of PV^+ and Stt^+ interneurons photostimulation was evaluated offline by measuring the following parameters in accepted stimulation protocol recordings. AP or EPSP potential latencies were defined as the time elapsed between electric stimulus onset and AP/EPSP peak time. AP or EPSP probabilities were calculated as the number of evoked AP/EPSP per number of electric stimulations and normalized across frequencies and cells. EPSP areas were quantified as the area between EPSP trace and baseline voltage level. EPSP amplitude was measured from baseline to peak. Output firing frequency was calculated based on the mean normalized AP probability.

2.4 Two-photon imaging

2.4.1 Head bar and cranial window implantation

2 to 4 weeks after injection, PV^+-Cre mice of both sexes injected with rAAV5/EF1α-DIO-hChR2(H123A)-mCherry-WPRE and AAV1-Syn-GCaMP6f-WPRE-SV40 were subcutaneously anaesthetized with a mix of ketamine (100 mg/kg) with medetomidin (0.14 mg/kg) and surgically implanted with a custom-made stainless steel head bar for head fixation (Figure 2.6-A). The dorsal surface of the skull was covered in cyanoacrylate adhesive followed by a layer of clean dental acrylic. The skull was then drilled above the barrel cortex to fit a 2.5 mm glass coverslip on the top of the injection sites of the virus stereotaxic injection. The glass coverslip was placed on the top of the brain and glued with cyanoacrylate adhesive.

During the whole surgical procedure and imaging, body temperature was monitored and maintained by a temperature control system (FHC Neuronal Microtargeting) and kept in light anaesthesia by subcutaneously injecting a mix of ketamine (50 mg/kg/h) with medetomidin (0.07 mg/kg/h).

2.4.2 Calcium-imaging

All calcium-imaging experiments were performed using a two-photon laser scanning B-Scope microscope (Thorlabs) with a femstosecond pulsed laser at 930 nm (Mai Tai Broadband, SpectraPhysics; 100 fs pulse width; 80 MHz repetition rate). The typical laser power was 20 to 35 mW (12 to 23% power setting). The isotropic fluorescence was collected with external photomultiplier tubes (Leica Microsystems). Morphology images were recorded in frame-scan mode (900 frames at 30 Hz each) with 10-line averaging using a 16x/0.8NA water immersion objective (Nikon). Images were acquired at zoom 4 (250x250 μm) with a resolution of 512x512 pixels.

2.4.3 Optogenetic stimulation

In photostimulation experiments, for half of the trials, a collimated 470 nm LED was used to generate wide field stimulation. Optogenetic stimulus consisted of a 3 s pulse of blue light (470 nm) applied right before the start of the image acquisition (30 s).

2.4.4 Sensory stimulation

To evoke sensory stimulation during imaging recordings, whiskers on the contralateral side of the cranial window implantation were deflected in a rostral-to-caudal-to-rostral direction during 18 s of the 30 s of recordings (3 repetitions of 2 s touching the whiskers with intervals of 4 s) by a vertical steel pole attached to a stepper motor controlled by open source hardware and software (Arduino) with a custom-made script. In half of the trials, neuronal activity was recorded without sensory stimulation and, in each case, combined with or without optogenetic stimulation as described above (Figure 2.6-B).

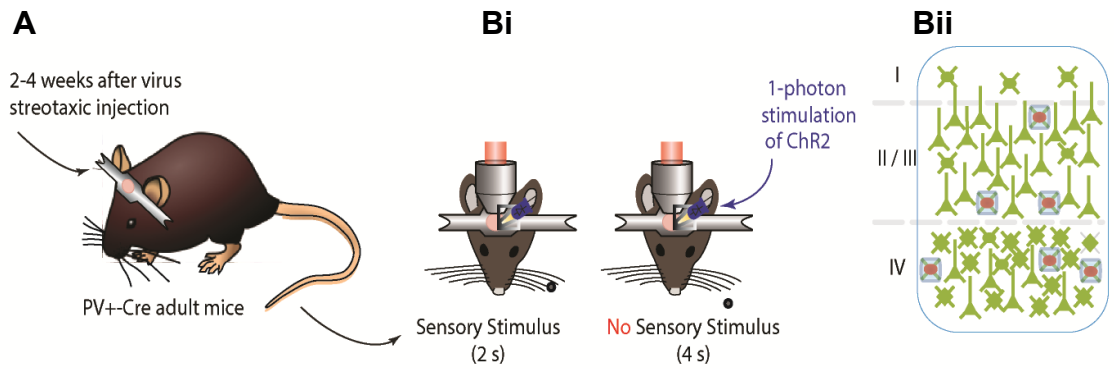

Figure 2.6. Two-photon imaging experiments simplified scheme. (A) A head bar and a cranial window were implanted in adult PV+-Cre mice 2 to 4 weeks after virus stereotaxic injection. **(Bi)** During two-photon imaging experiments combined with photostimulation, mice were repeatedly stimulated with a vertical steel pole (repetitions of 2 s touching the whiskers with intervals of 4 s). **(Bii)**Neuronal activity was recorded from neurons expressing GCaMP (green neurons) and photostimulation (blue squares) was permitted due to expression on PV+ neurons expressing channelrhodopsin 2 (**ChR2**; red neurons).

2.4.5 Histology

After termination of the recordings, mice were deeply anesthetized with a mix of ketamine (200 mg/kg) with medetomidin (0.28 mg/kg) and transcardially perfused with 4% paraformaldehyde solution. Brains were post-fixed overnight at 4 °C in the same solution, which was then replaced by a 0.1 M PBS solution. 80 µm thick coronal sections were cut in ice-cold 0.1 M PBS using a semi-automated vibratome (VT1000S, Leica). Slices were mounted in vectashield mounting medium (Vector Labs) and imaged with a laser scanning confocal microscope (FV1000, Olympus) equipped with an air 20x/0.75NA.

2.4.6 Data analysis

Recorded images of activity were motion-corrected off-line using TurboReg (Thevenaz et al., 1998) and analysed with Caltracer3 Beta (Rafael Yuste's Lab, Columbia University, USA) and custom-written scripts executed in Matlab (Mathworks).

For calculation of the relative change in fluorescence (ΔF/F0), regions of interest (ROIs) for somas and dendrites were automatically detected with a custom-written software executed in Matlab (Mathworks) and manually adjusted afterwards. Somatic and dendritic signals were calculated as the mean pixel

intensity of the pixels in the ROI. The surround signal was calculated for each frame as the mean intensity of pixels. The soma or dendrite/surround ratio was then calculated for each frame. Excitation out of the soma was correct by neuropil subtraction. The somatic and dendritic fluorescence was divided by fluorescence signals measured from nearby neuropil, producing for each neuron a regression coefficient valued in ΔF/F0.

To analyse changes in activity across the different conditions, I calculated the mean ΔF/F0 in a 7 s window right after a period with or without photostimulation (mean_opto) and a 7 s window at the end of the trace, where there was no stimulation present (mean_ctrl) or where there was evoked sensory stimulation without photostimulation (mean_stim). The difference between the two means was used to quantify the change in network activity (Figure 2.7).

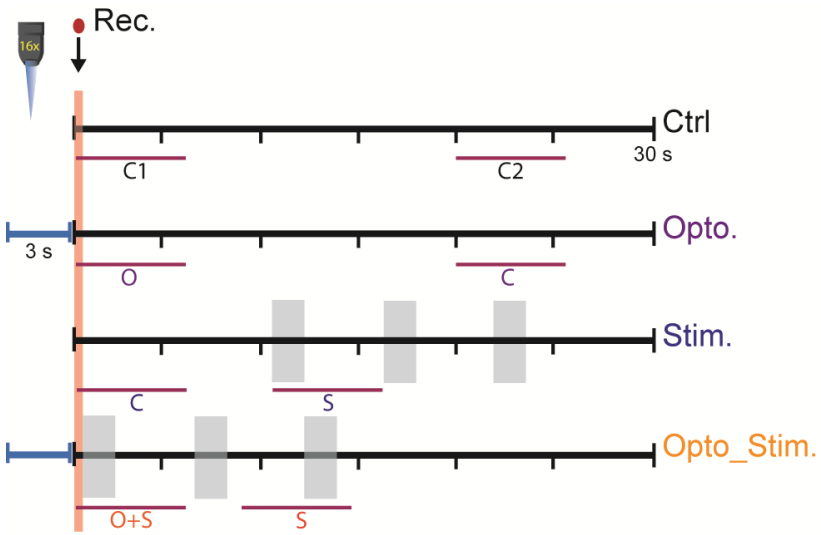

Figure 2.7. Two-photon imaging time windows used to ΔF/F0 calculate variance across different conditions. In each condition two representative recording time windows of 7 s were defined within a period of time of 30 s. During analysis in control condition (**Ctrl**), two control windows (**C1** and **C2**) were defined and compared. In experiments with photostimulation only (**Opto.**) it was analysed activity right after the optogenetic stimulation (**O**; blue bar) and a control period towards the end of recording (**C**). To analyse sensory stimuli effect (**Stim., vertical grey bar**), a window where not stimulus were applied was compared with a period where mice whiskers were stimulated (**S**). In experiments in which photostimulation was combined with sensory stimulus (Opto_Stim.), a time window of sensory stimulation combined with optogenetics (O+S) was compared with a time window in which only sensory stimulation was being applied.

2.5 Statistical analysis

Data was analysed using the graphing and analysis package Graphpad Prism (Graphpad). Electrophysiological properties of neurons were analysed calculating mean and standard-deviation (SD). Effect of optogenetic stimulation *in vitro* and effect of optogenetic and sensory stimulation *in vivo* were analysed calculating the mean and standard-error of the mean (SEM). Differences between means were analysed with the parametric statistical test one-way ANOVA and multicomparisons corrected using with Sidak's multiple comparisons test. p-values less than 0.05 were considered significant.

Chapter III

Results

3.1 Validation of an optogenetic approach for neuronal-type specific activity manipulation and recording

The vibrissal somatosensory system has been extensively used in studies that aim to elucidate somatosensory processing principles. Amongst other features, the rodent primary somatosensory system is relatively simple, easy to manipulate and has a highly organised barrel cortex columns-whiskers associative map (Nicolelis and Ribeiro, 2006, Petersen, 2007). Additionally, because of the possibility of combining molecular tools with the wide variety of available transgenic strains (Petersen, 2009), mice are considered a very attractive model to study mammal physiology. Particularly, in the neuroscience field, the use of genetically targeted actuators and indicators (e.g. opsins and calcium indicators) allows us to manipulate and record activity of genetically defined neuronal populations with very precise control by (Luo et al., 2008, Scanziani and Hausser, 2009).

The success of this project required the precise control of activity of two genetically defined populations of inhibitory neurons, somatostatin and parvalbumin-expressing neurons, through the use of genetically targeted actuators (i.e. Channelrhodopsin 2). This level of genetic targeting could only be achieved through the use of the Cre-lox system for targeted genetic recombination. To achieve cell-type specific expression of opsins and calcium indicators I used viral vectors too deliver optogenetic constructs flanked by loxP sites into the brain of PV^{+}-Cre and Stt^{+}-Cre transgenic mice. These mice strains express the enzyme Cre recombinase under the promotor of parvalbumin or somatostatin, respectively. Thus, allowing the expression of channelrhodopsin 2 specifically in parvalbumin and somatostatin-expressing GABAergic neurons (Luo et al., 2008, Scanziani and Hausser, 2009, Sachidhanandam et al., 2013).

3.1.1 Establishment of homozygous transgenic colonies

In order to achieve the necessary expression specificity of optogenetic actuators and indicators, as mentioned above, it was necessary to firstly establish homozygous colonies of PV^{+}-Cre and Stt^{+}-Cre mice strains. To increase reproducibility of the results obtained, in both cases I took the care to avoid substrains and prevent genetic drift from the original commercial stock colony.

Thus, our PV^{+}-Cre mice colony was established by using breeders from a recently established transgenic homozygous colony. Additionally, I established a homozygous colony of Stt^{+}-Cre mice after mating genotyping-positive homozygous (Stt$^{+\text{-Cre}}$ / Stt$^{+\text{-Cre}}$), selected from a F1 litter obtained by crossing a pair of recently acquired heterozygous (Stt$^{+\text{-Cre}}$ / Stt$^{\text{-WT}}$) transgenic breeders (Figure 3.1). Brain slices obtained for electrophysiology experiments of all animals of one F2 litter were revealed positive for channelrhodopsin2-mCherry expression (Figure 3.2). This could only occur in transgenic mice through Cre-mediated recombination, thus confirming the success of the establishment of the homozygous colony.

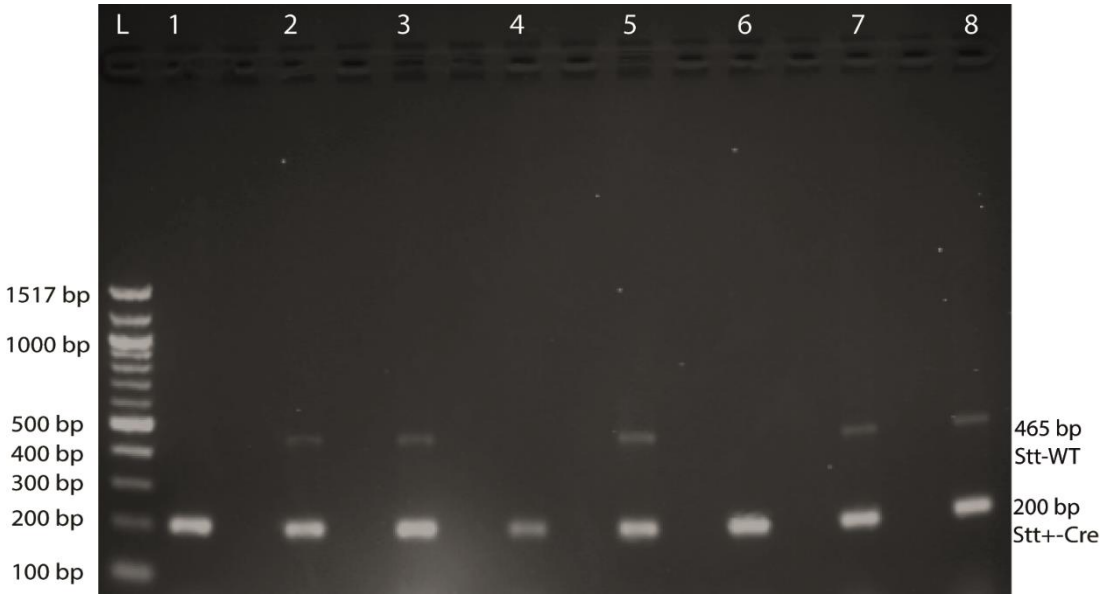

Figure 3.1. Homozygous Stt^{+}-Cre mice were identified through genotyping. Distinct forward primers were used for amplification of wild type (Stt-WT; 465 bp) and mutant (Stt^{+}-Cre; 200 bp) alleles fragments. Identified homozygous transgenic animals (1, 4 and 6) were selected as breeders for the establishment of a transgenic Stt^{+}-Cre colony. It was used a 100 bp DNA ladder (**L**).

3.1.2 Assessment of hChR2 or GCaMP6f expression in neurons of interest in the barrel cortex

With the purpose of obtaining precise activity control with high temporal resolution of PV^{+} and Stt^{+} interneurons, transgenic mice of established PV^{+} and Stt^{+}-Cre were transfected with channelrhodopsin 2, a light-gated non-selective cationic membrane channel. Thus, before conducting electrophysiological experiments, which would involve the manipulation of the two interneurons, the expression of ChR2 was assessed in these cells. Immunohistochemistry analysis of injected mice brain slices revealed co-localization of parvalbumin with mCherry

(Figure 3.2 – A) and somatostatin with eYFP (Figure (3.2–B). mCherry and eYFP expression were, together with ChR2, double-floxed and inverted in the respective vectors. Accordingly, the expression of these fluorescent proteins observed in the respective immunohistochemistry results confirm the success of the cre-mediated recombination in the interneurons of interest in the mouse barrel cortex of both, PV^{+} and Stt^{+}-Cre, transgenic trains.

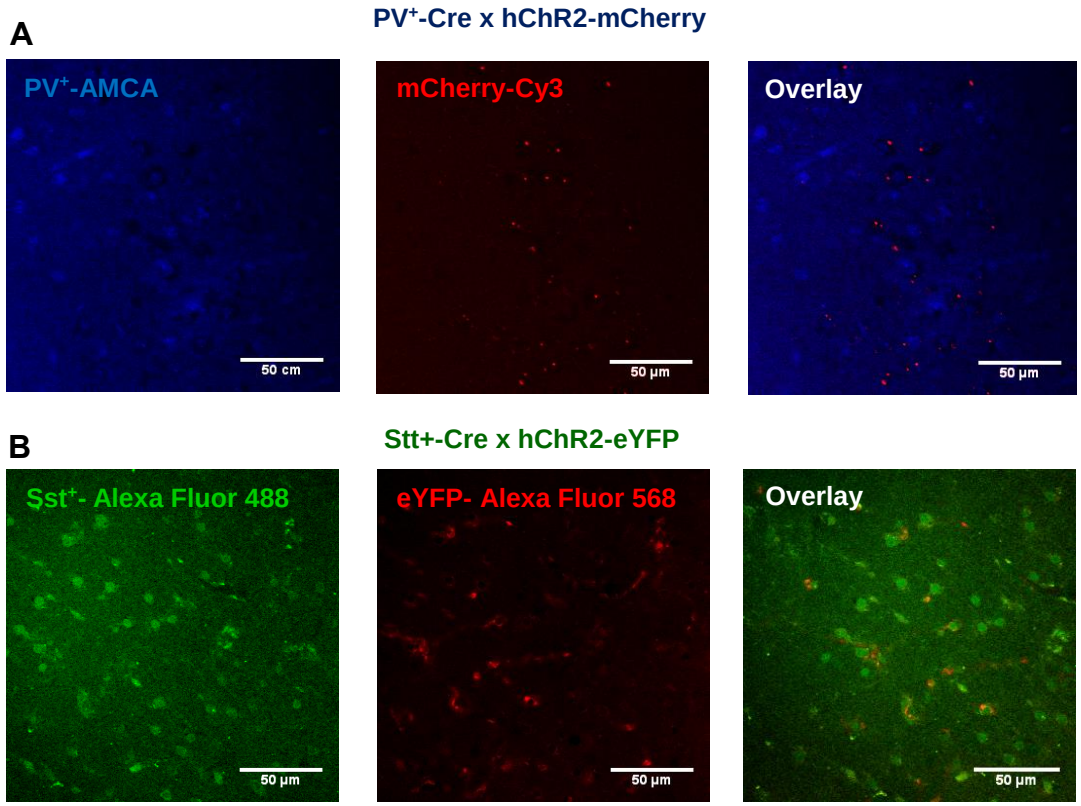

Figure 3.2. hChR2 co-localizes with parvalbumin (PV^{+}) - or somatostatin-expressing (Stt^{+}) GABAergic neurons in the barrel cortex of injected PV^{+}-Cre and Stt^{+}-Cre mice, respectively. Virus with double-floxed inverted humanized version of channelrhodopsin 2 (**hChR2**) coupled to mcherry or yellow fluorescent protein (**eYFP**) were injected in PV^{+}-Cre or Stt^{+}-Cre mice, respectively. **(A)** Thalamocortical brain slices from PV^{+}-Cre animals, 4 to 8 weeks after injections, were fixed and stained against parvalbumin and mCherry. Signal was enhanced with aminomethylcoumarin (**AMCA**) (blue) and Cy3 (red), respectively. **(B)** Thalamocortical brain slices obtained from Stt^{+}-Cre animals, 4 to 6 weeks after injections, were fixed and stained against somatostatin and eYFP. Signal was enhanced with Alexa Fluor 488 (green) and Alexa Fluor 568 (red), respectively.

In order to evaluate the effect of optogenetic stimulation of PV^{+} INs in the activity of neuronal populations of the mice barrel cortex in *vivo*, together with the optogenetic actuator ChR2, I used a fast version of the genetically encoded calcium

indicator GCAMP6 (GCAMP6f). Thus, before initiating calcium-imaging experiments combined with optogenetic stimulation of PV^+ interneurons, the expression of ChR2 and GCaMP6f was assessed with histology experiments. The expression of both optogenetic tools was observed in the barrel cortex of brain slices of injected PV^+-Cre mice (Figure 3.3). Therefore, confirming the success of the virus transfection and cre-mediated recombination of ChR2-mCherry in the barrel cortex of these animals.

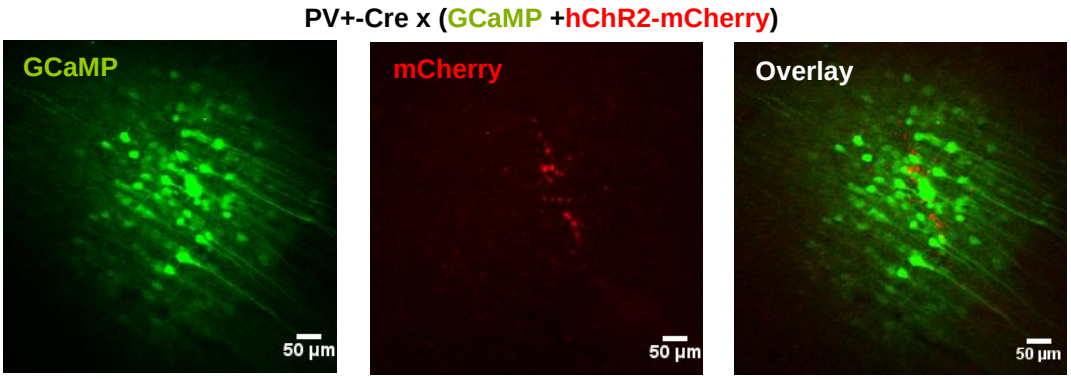

Figure 3.3. GCaMP6f and hChR2 are expressed in the barrel cortex of injected PV^+-Cre mice. A mix of virus with a double-floxed inverted humanized version of channelrhodopsin 2 (hChR2) coupled to mcherry (red) and a fast version of the genetically encoded calcium indicator GCaMP6 (GCaMP6f; green) were injected in PV^+-Cre. 2 to 4 weeks after viral injections, mice were perfused and barrel-cortex containing coronal slices were mounted and visualized without signal enhancement.

In order to better plan further calcium-imaging experiments, the location of GCaMP6f expression in each layer of the barrel cortex was also assessed by histology. Expression of this optogenetic reporter was mainly observed in layer 2/3(Figure 3.4). GCaMP6f was poorly expressed in the remaining cortical layers. Additionally, with this histology experiment I observed, in coronal brain slices, axons from neurons in the barrel cortex expressing GCaMP6f projecting through the striatum, in direction to the thalamus.

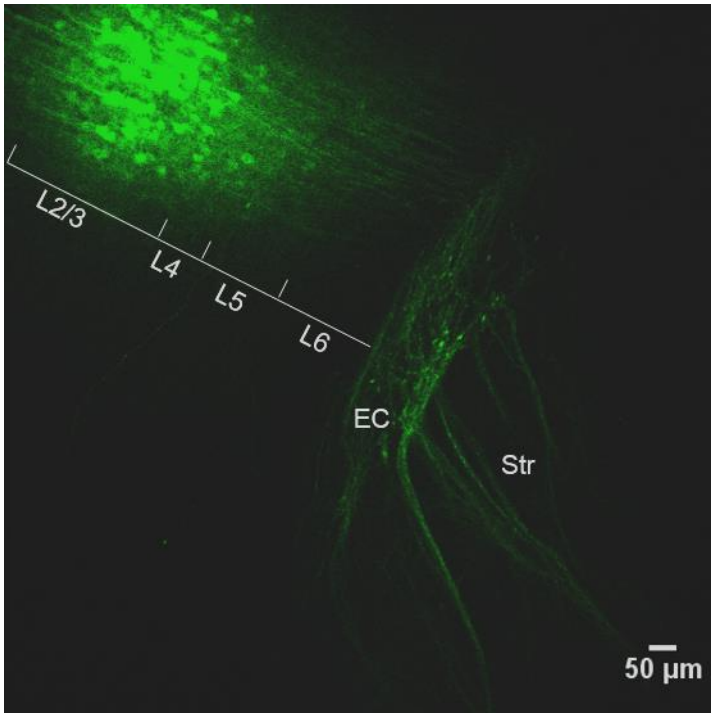

Figure 3.4. GCaMP6f is expressed in mainly expressed in layer 2/3 of the barrel cortex. The expression of a fast version of the genetically encoded calcium indicator GCAMP6 (GCaMP6f; green) in the barrel cortex was assessed in barrel cortex-containing brain slices of PV$^+$-Cre mice, perfused after two-photon imaging experiments, without signal enhancement. GCaMP6f is mainly expressed in neurons in layer 2/3 of the barrel cortex. Axons from some cells in the barrel cortex expressing GCaMP6f have projections in direction to the thalamus, through the striatum (**Str**). **EC** – external capsule; **L4** –layer 4; **L5** – layer 5; **L6** – layer 6.

With these results, the proposed optogenetic approach for cell-type specific activity manipulation (expression of ChR2 in PV$^+$ and Stt$^+$ neurons) and monitoring (non-specific expression of GCaMP6f) was established and further experiments initiated.

3.2 Effect of PV$^+$ and Stt$^+$ INs photostimulation in synaptic transmission *in vitro*

Inhibition seems to have an essential role in sensory processing. PV$^+$ and Stt$^+$ interneurons, two of the more abundant inhibitory neurons in the cortex(Rudy et al., 2011), are likely to distinctly contribute for synaptic transmission processes during sensory stimulation. The thalamus works receives the majority of the afferent somatosensory information, retransmitting it mainly into layer 4 of the barrel cortex, which in turn relays into layer 2/3 (Bastos et al., 2012). Thus, in

order to study the distinct effect of PV^+ and Stt^+ interneurons in somatosensory processing, electrophysiological recordings with electric stimulation in the internal capsule were performed in combination with cell-specific optogenetic manipulation of PV^+ and Stt^+ interneurons. Electric stimulation in the internal capsule was used before to study thalamocortical projections into the barrel cortex (Agmon and Connors, 1991).

3.2.1 Electrophysiological properties of cells in layers 2/3 and 4 of the barrel cortex

In order to characterise and identify the type of cells in layer 2/3 and 4 of the barrel cortex in which electric and optogenetic stimulation protocols were performed, the electrophysiological properties of these cells were analysed. This information was obtained offline by analysis of a -200 to +200 pA current-steps protocol performed before the recording of the electric stimulation protocols.

The analysis of current injection–evoked firing patterns permitted the identification of five main neuronal types (Figure 3.5). The characteristics of these cells allowed identification of neuronal sub-types in accordance with previous literature (Ascoli et al., 2008, Young and Sun, 2009, Chen et al., 2015). I identified three types of INs: a fast-spiking (FS) neuron, by its high firing frequency and low interspike interval adaption (Figure 3.5 – A); an irregular spiking GABAergic neuron, by its irregular spiking (Figure 3.5 – B); a non-fast spiking slow-adapting (NFSA), GABAergic neuron by its high interspike interval adaptation (Figure 3.5 – C).

Two types of excitatory cells were also distinguished amongst the current-step evoked firing patterns. Discrimination between excitatory pyramidal and spiny stellate cells is not possible based solely on electrophysiological parameters However, differences in the onset of the first action potential and in the repolarization phases, have been previously used to distinguish between late (LS) and early spiking (ES) excitatory neurons (Figure 3.5 – D, E) (Cowan and Stricker, 2004, Lopez de Armentia and Sah, 2004).

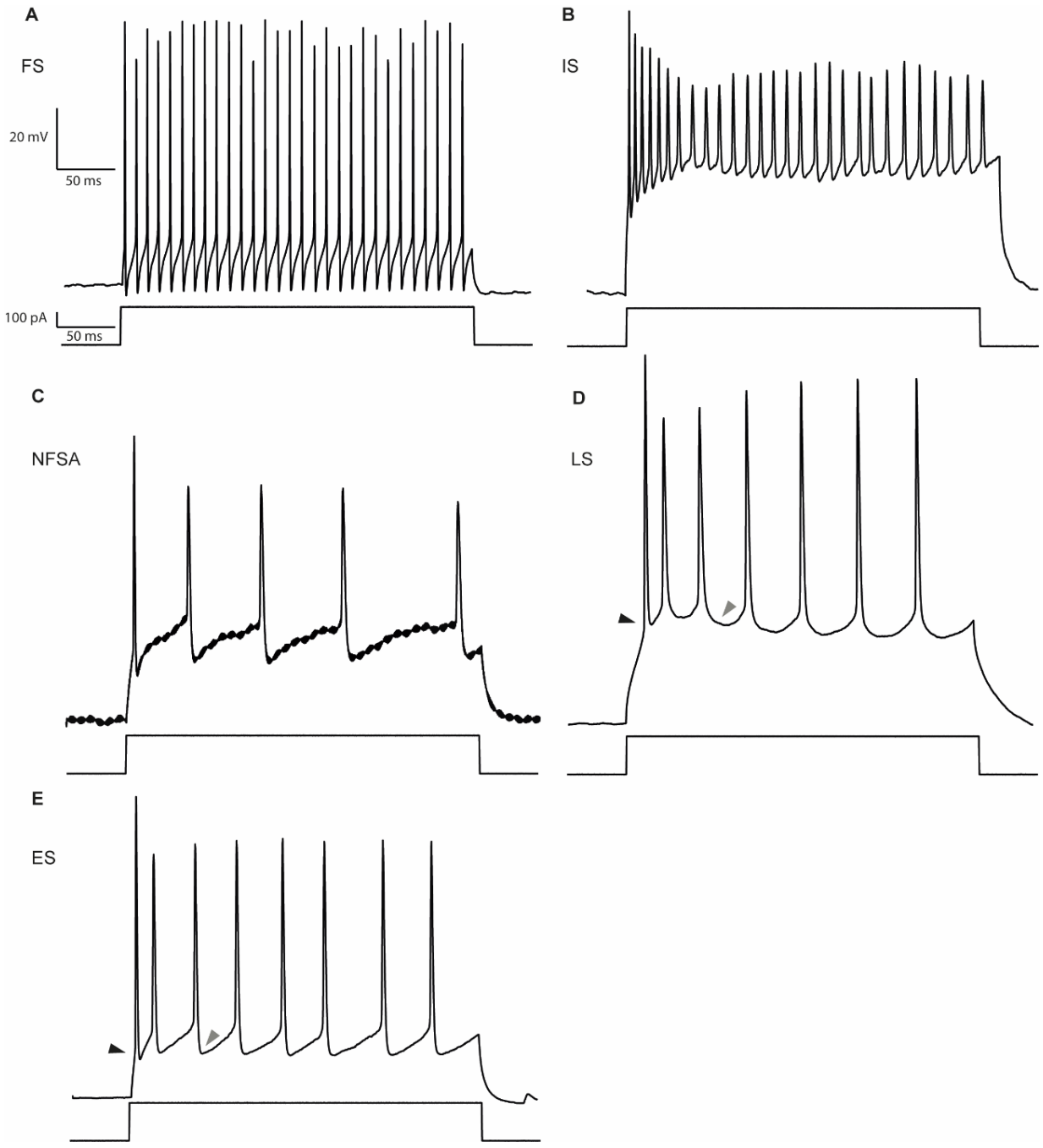

Figure 3.5. Representative current-evoked firing patterns of cells in layer 2/3 and 4 of the barrel cortex. Representative membrane responses of **(A)** a fast-spiking GABAergic neuron (**FS**), **(B)** an irregular spiking GABAergic neuron (**IS**), **(C)** a non-fast spiking slow-adapting GABAergic neuron (**NFSA**), **(D)** a late spiking excitatory neuron (**LS**) and **(F)** an early spiking excitatory neuron (**ES**), to current injections of 200 pA. The difference between the last two is denoted by the arrows on the figure pointing to the onset of the first action potential (**black arrows**) and the differences in the repolarization phase (grey arrows).

Additionally, some of the most commonly measured electrophysiology properties were obtained from the current-steps evoked-firing patterns: action potential amplitude, action potential half-width, firing frequency, input resistance, interspike interval adaptation, resting membrane potential, and rehobase. 3.1

summarizes information of these electrophysiology properties. Only one cell from both IS and NFSA neurons subtypes were recorded. Thus, PV^+ neurons refer to fast spiking interneurons (FS) (Figure 3.5 – A), while excitatory (Exc.) cells includes late (LS) and early (ES) spiking neurons (Figure 3.5 – D, E). The distribution of cells from which recordings were obtained is in accordance with the proportion of interneurons versus excitatory cells existent in cortical layers (around 15% of INs) (Ascoli et al., 2008).

Table 3.1. Electrophysiological properties of parvalbumin-expressing INs (PV^+) and excitatory neurons (Exc.) in layers 2/3 and 4 of the barrel cortex.

Properties	Exc. L2/3	PV^+ L2/3	Exc. L4	PV^+ L4
AP amplitude (mV)	72.77 ± 22.85 (n=16)	64.64 ± 2.8 (n=3)	79.15 ± 15.46 (n=37)	72.78 ± 10.3 (n=5)
AP half-width (ms)	2.13 ± 0.98 (n=16)	0.6 ± 0.43 (n=3)	1.63 ± 0.63 (n=33)	0.54 ± 0.25 (n=5)
Firing frequency (Hz)	19.77 ± 22.9 (n=16)	88.16 ± 31.15 (n=3)	21.64 ± 9.1 (n=32)	80.8 ± 19.6 (n=5)
Input resistance (MΩ)	234.9 ± 129.4 (n=9)	250.7 ± 231.7 (n=3)	193.9 ± 139.5 (n=29)	227.96 ± 108.8 (n=5)
Interspike interval adaptation (ms)	30.92 ± 12.1 (n=16)	3.01 ± 4.6 (n=3)	35.6 ± 17.6 (n=37)	17.64 ± 1.78 (n=5)
Resting membrane potential (mV)	-74.40 ± 6.27 (n=20)	-66.50 ± 2.121 (n=2)	-67.4375 ± 3.54 (n=16)	-64.25 ± 2.99 (n=5)
Rheobase (pA)	96.92 ± 52.5 (n=13)	66.67 ± 28.86 (n=3)	100 ± 52.7 (n=37)	112.5 ± 62.9 (n=5)

To confirm a correct segregation of these neuronal types, I plotted a distribution based on action potential half-width (Figure 3.6) and firing frequency (Figure 3.7) of putative excitatory and fast spiking PV^+ neurons in layers 2/3 and 4 of the barrel cortex. These distributions confirmed the previous classification based on the evoked firing patterns (Young and Sun, 2009, Avermann et al., 2012).

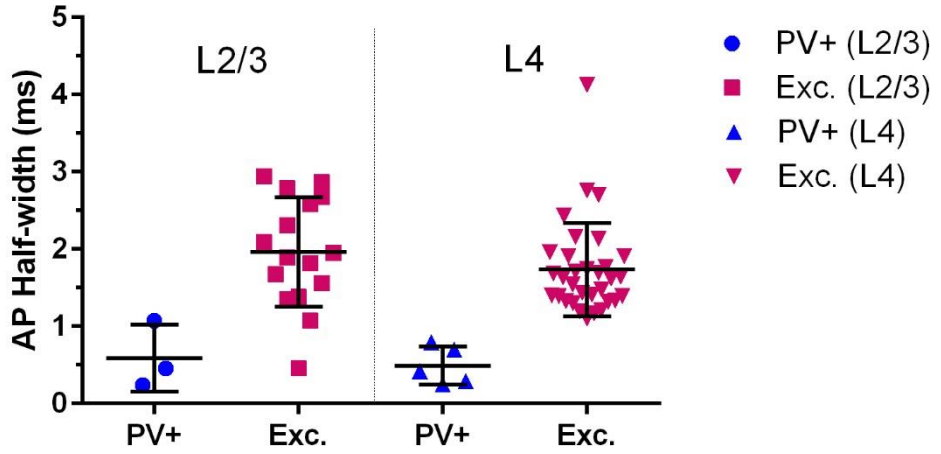

Figure 3.6. AP half-width distribution of parvalbumin-expressing INs and excitatory neurons in layers 2/3 and 4 of the barrel cortex. Data was grouped according the type of neuron, parvalbumin-expressing INs (**PV+**) or excitatory neurons (**Exc.**), and per layer, layers 2/3 (**L2/3**) or 4 (**L4**) of the barrel cortex. Represented is mean ± SD. PV^+ in L2/3, 0.56 ± 0.43 ms; n=3; Exc. in L2/3: 1.96 ± 0.70 ms, n=16; PV^+ in L4: 0.54 ± 0.25 ms; n=5; Exc. in L4: 1.74 ± 0.60 ms, n=32.

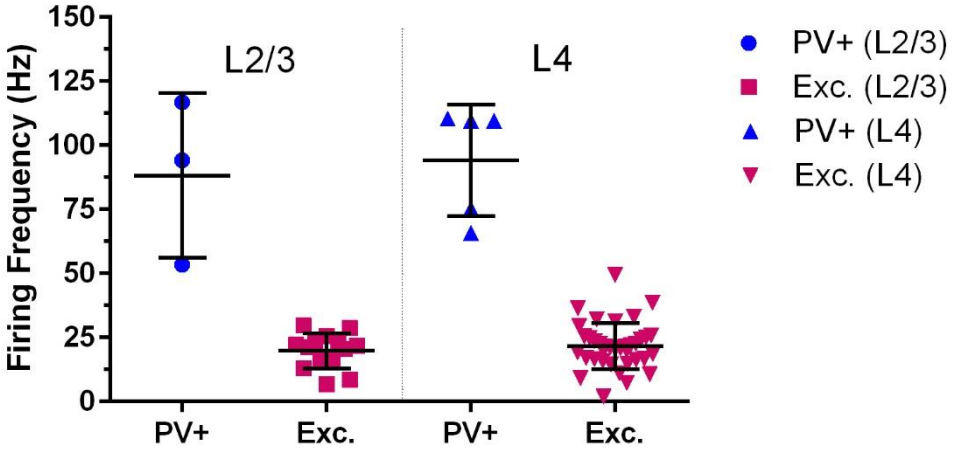

Figure 3.7. Firing frequency of parvalbumin-expressing INs and excitatory neurons in layers 2/3 and 4 of the barrel cortex. Data was grouped according the type of neuron, parvalbumin-expressing INs (**PV+**) or excitatory neurons (**Exc.**), and per layer, layers 2/3 (**L2/3**) or 4 (**L4**) of the barrel cortex. Represented is mean ± SD. PV^+ in L2/3: 88.16 ± 32.15 Hz, n=3; Exc. in L2/3: 19.76 ± 6.83 Hz, n=16; PV^+ in L4: 94.16 ± 21.79 Hz, n=5; Exc. in L4: 21.64 ± 9.10 Hz, n=32.

Additionally, neuronal identity was confirmed by immunohistochemistry of cells filled with biocytin during electrophysiological recordings. Figure 3.8 shows a representative excitatory cell (Spruston, 2008).

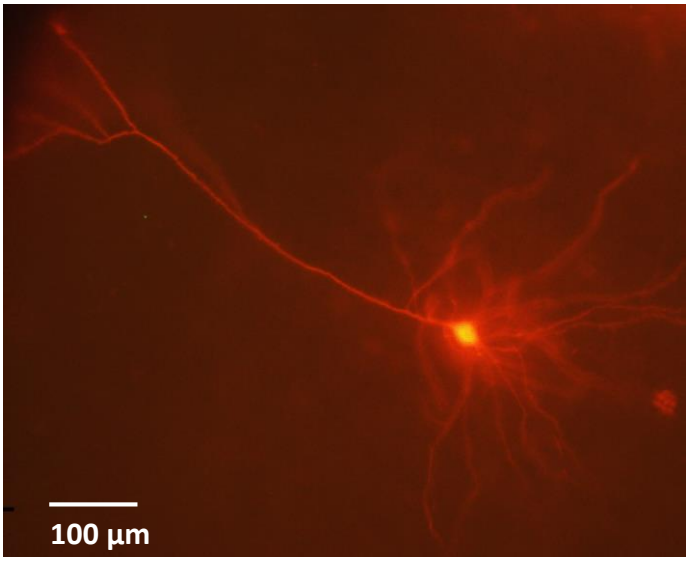

Figure 3.8. Representative excitatory cell of layer 4 of the barrel cortex. During electrophysiological recordings cells were filled with biocytin. Brain slices were fixed and stained with Texas Red Avidin D.

3.2.2 Effect of PV+ and Stt+ INs photostimulation in synaptic transmission in layers 2/3 and 4 of the barrel cortex

To evaluate the effect of PV+ and Stt+ INs activation on synaptic transmission of thalamocortical inputs into excitatory neurons, I performed current-clamp electrophysiological experiments. Thalamocortical responses, electrically evoked in the internal capsule, were recorded in cells of layers 2/3 and 4 of the barrel cortex. To observe the effect of PV+ optogenetic stimulation at different input frequencies I used 5 distinct frequencies (2, 5, 10, 20 and 30 Hz) in combination with photostimulation.

To assess the effect of optogenetic stimulation of PV+ and Stt+ INs, evoked excitatory postsynaptic potentials (EPSPs) latency (ms), area (mV/ms) and amplitude (mV) were analysed. Additionally, evoked action potentials (APs) latency (ms), probability and frequency (Hz) were calculated. These measurements were then compared across neuronal populations between blue (470 nm) light ON and light OFF conditions.

In layer 4 excitatory cells, evoked EPSPs latency differences between PV+ light ON and light OFF were not observed in any stimulation frequency (Figure 3.9–A). EPSPs areas were also similar between conditions across stimulation frequencies (Figure 3.9–B). Amplitude of EPSPs varied between light ON and light OFF

conditions but changes were not systematic across frequencies (Figure 3.9–C). Therefore, as shown in the example traces in Figure 3.9–D, optogenetic stimulation of PV⁺ neurons does not seem to affect evoked EPSPs in layer 4 of the barrel cortex.

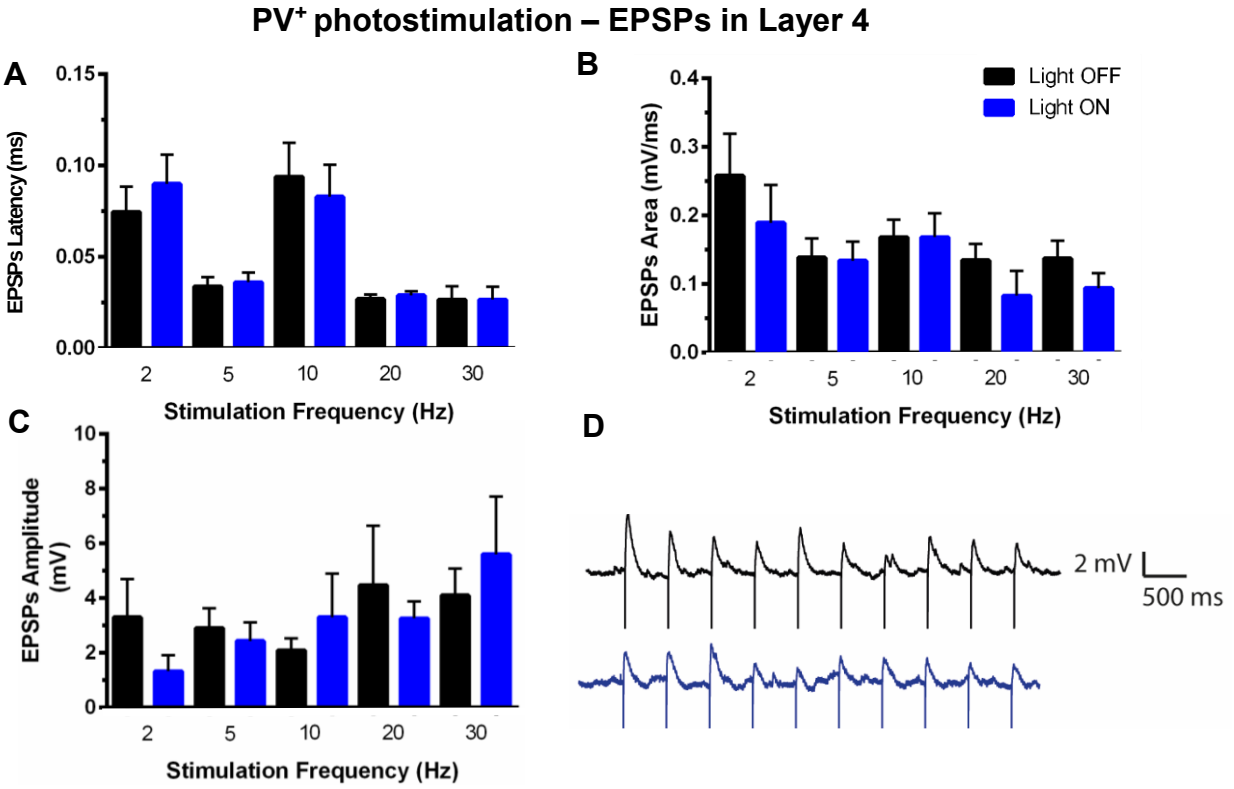

Figure 3.9. PV⁺ INs optogenetic stimulation does not affect evoked EPSPs in layer 4 of the barrel cortex. Thalamocortical stimulation responses were recorded using ten electric stimulation protocols with 5 different frequencies (2, 5, 10, 20 and 30 Hz) in thalamocortical brain slices of PV⁺-Cre mice injected with double-floxed inverted hChR2, 4 to 8 weeks after injections. Recordings were also performed in combination with optogenetic stimulation in half of the trials. **(A)** Excitatory postsynaptic potentials (EPSPs) latency (ms), **(B)** area (mV/ms) and **(C)** amplitude (mV) were measured and compared between light ON and light OFF conditions. Data was grouped by frequency and condition. Represented is mean ± SEM; n=13 cells; there were no statistically significant comparisons. Data was analysed with parametric statistical test one-way ANOVA and multicomparisons corrected using with Sidak's multiple comparisons test. **(D)** Example of evoked EPSP traces at 5 Hz in light ON and light OFF conditions.

Action potentials recorded from excitatory cells in layer 4 exhibited very low latency, close to 0 ms, in all the stimulation frequencies either in PV⁺ light ON and light OFF conditions (Figure 3.10–A). However, although differences are not statistical significant, AP probability was lower when PV⁺ neurons were photostimulated in all stimulation frequencies (Figure 3.10–B). These differences were also observed when spiking frequencies were plotted against the different

stimulation frequencies used (Figure 3.10–C). Thus, as observed in the example traces of Figure 3.10–D, optogenetic stimulation of PV⁺ INs seems to decrease the number of action potentials in excitatory cells in layer 4 of the barrel cortex.

Figure 3.10. PV⁺ INs optogenetic stimulation reduces evoked spikes frequency in layer 4 of the barrel cortex. Thalamocortical stimulation responses were recorded using ten electric stimulation protocols with 5 different frequencies (2, 5, 10, 20 and 30 Hz) in thalamocortical brain slices of PV⁺-Cre mice injected with double-floxed inverted hChR2, 4 to 8 weeks after injections. Recordings were also performed in combination with optogenetic stimulation in half of the trials. **(A)** Action potentials (APs) latency (ms), **(B)** probability and **(C)** frequency were measured and compared between optogenetic stimulation and control conditions. Data was grouped by frequency and condition. Represented is mean ± SEM: n=13 cells; there were no statistically significant comparisons. Data was analysed with parametric statistical test one-way ANOVA and multicomparisons corrected using with Sidak's multiple comparisons test. **(D)** Example of evoked AP traces at 5 Hz in light ON and light OFF conditions.

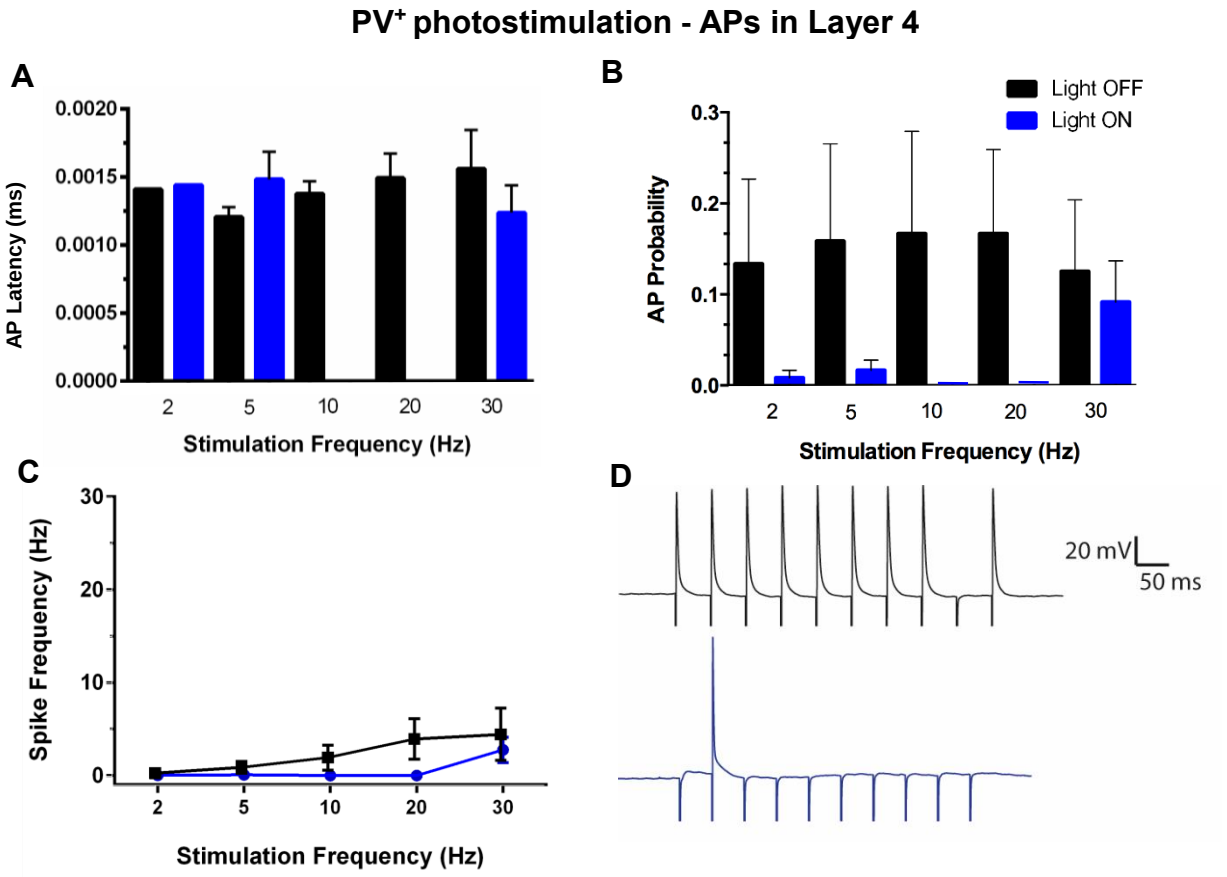

In layer 2/3 of the barrel cortex it was not possible to observe evoked EPSPs, only action potentials: electric stimulation in internal capsule appears to trigger only all-or-none responses in excitatory cells of L2/3.

Action potentials recorded from excitatory cells in L2/3 exhibited very low latency, close to 0 ms, in all the stimulation frequencies either in light ON and light OFF conditions (Figure 3.11–A).

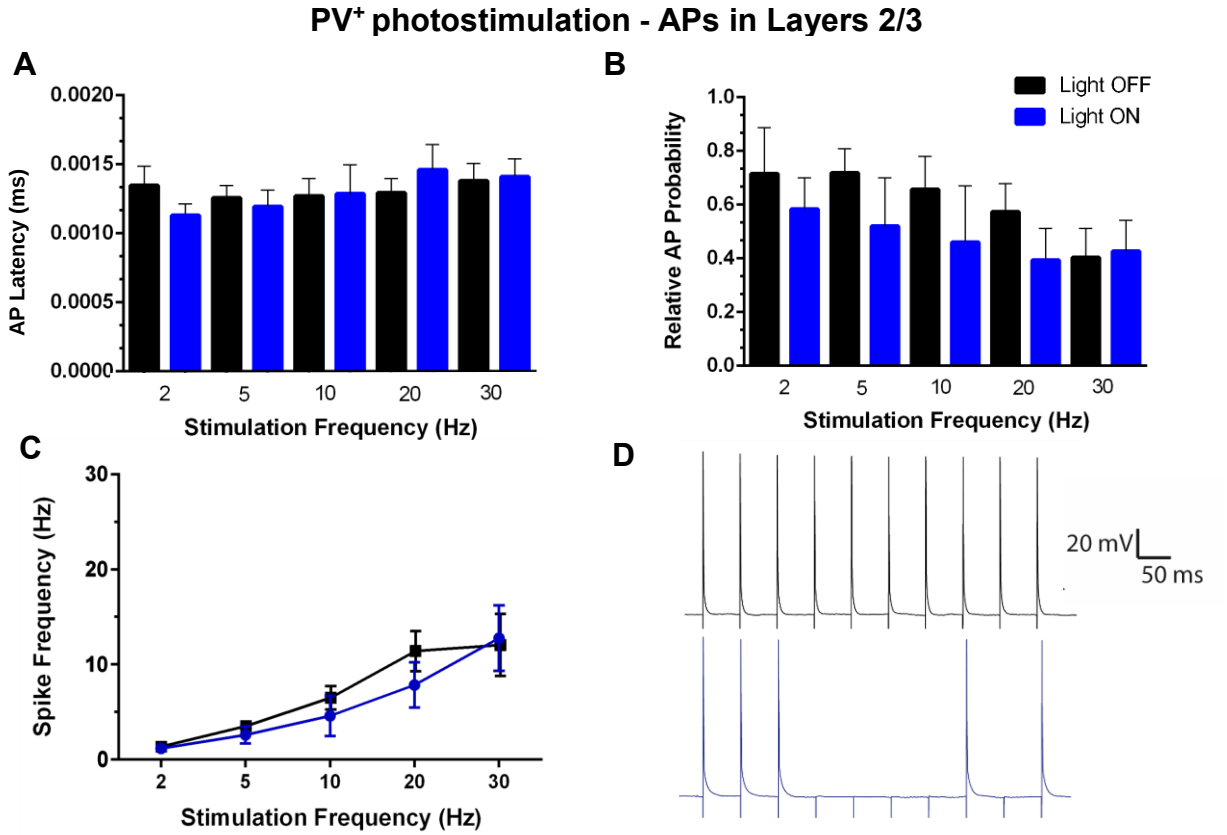

Figure 3.11. PV+ INs optogenetic stimulation reduces evoked spikes frequency in layer 2/3 of the barrel cortex. Thalamocortical stimulation responses were recorded using ten electric stimulation protocols with 5 different frequencies (2, 5, 10, 20 and 30 Hz) in thalamocortical brain slices of PV+-Cre mice injected with double-floxed inverted hChR2, 4 to 8 weeks after injections. Recordings were also performed in combination with optogenetic stimulation in half of the trials. **(A)** Action potentials (APs) latency (ms), **(B)** probability and **(C)** frequency were measured and compared between optogenetic stimulation and control conditions. Data was grouped by frequency and condition. Represented is mean ± SEM, n=5 cells; there were no statically significant comparisons. Data was analysed with parametric statistical test one-way ANOVA and multicomparisons corrected using with Sidak's multiple comparisons test. **(D)** Example of evoked AP traces at 5 Hz in light ON and light OFF conditions.

Cells recorded in layer 2/3 displayed very different output firing frequencies, action potential probabilities were normalised per cell across firing frequencies and then per population, separately for light ON and light OFF conditions. Even though differences observed in the normalised action potential probabilities

between light ON and light OFF conditions, AP probability was lower when PV^+ neurons were photostimulated stimulation frequencies of 2, 5, 10 and 20 Hz (Figure 3.11–B). At a stimulation frequency of 30 Hz no difference was observed in AP probability between light ON and light OFF conditions (Figure 3.11–B). This was also observed when spiking frequencies were plotted against the different stimulation frequencies used (Figure 3.11–C). Accordingly, as observed in the example traces of Figure 3.11–D, optogenetic stimulation of PV^+ INs seems to decrease the number of action potentials in excitatory cells in layer 2/3 of the barrel cortex.

In evoked EPSPs of excitatory cells of Stt^+-Cre mice brain slices, the three measured parameters, latency, area and amplitude varied between light ON and light OFF conditions but changes were not systematic across frequencies (Figure 3.12–A, B and C, respectively). Therefore, as observable in the example traces in Figure 3.12–D, optogenetic stimulation of Stt^+ neurons does not show a systematic effect on evoked EPSPs in layer 4 of the barrel cortex.

When looking at evoked-action potentials recorded from excitatory cells in layer 4 properties, latency was very low, close to 0 ms, in all the stimulation frequencies either in Stt^+ optogenetic stimulation or control conditions (Figure 3.13–A). As cells recorded in this layer displayed very different output firing frequencies, action potential probabilities were normalized per cell across firing frequencies and then per population, separately for optogenetic stimulation and control conditions. AP probabilities varied between optogenetic stimulation and control conditions but changes were not systematic across frequencies (Figure 3.13–B). Looking at spike frequencies obtained across the different stimulation frequencies, optogenetic stimulation of Stt^+ interneurons optogenetic stimulation does not seem to have a systematic or significant effect on evoked action potentials on layer 4 of the barrel cortex. This is also illustrated in the example traces in Figure 3.13–D.

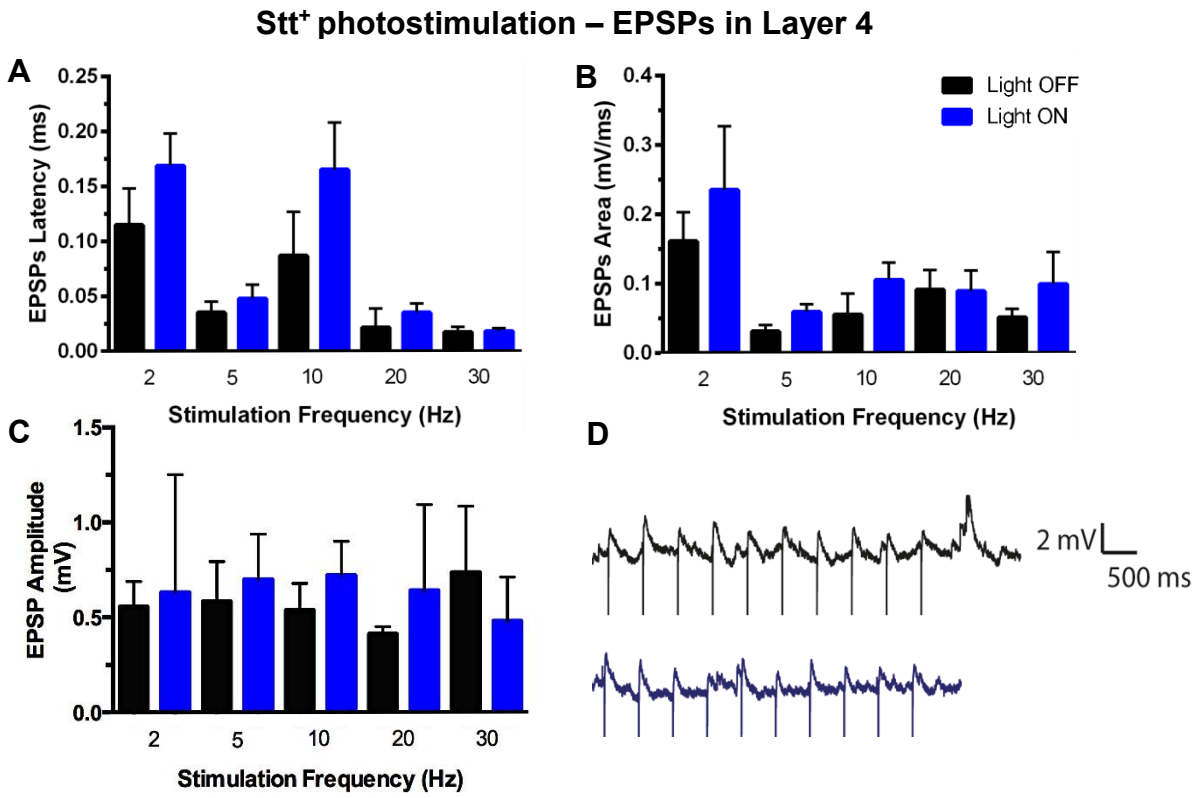

Figure 3.12. Stt⁺ INs optogenetic stimulation does not affect evoked EPSPs in layer 4 of the barrel cortex. Thalamocortical stimulation responses were recorded using ten electric stimulation protocols with 5 different frequencies (2, 5, 10, 20 and 30 Hz) in thalamocortical brain slices of Stt⁺-Cre mice injected with double-floxed inverted hChR2, 4 to 6 weeks after injections. Recordings were also performed in combination with optogenetic stimulation in half of the trials. **(A)** Excitatory postsynaptic potentials (EPSPs) latency (ms), **(B)** area (mV/ms) and **(C)** amplitude (mV) were measured and compared between optogenetic stimulation and control conditions. Data was grouped by frequency and condition. Represented is mean ± SEM, n=8 cells; analysed with Sidak's multiple comparisons test. **(D)** Example of evoked EPSP traces at 5 Hz in light ON and light OFF conditions.

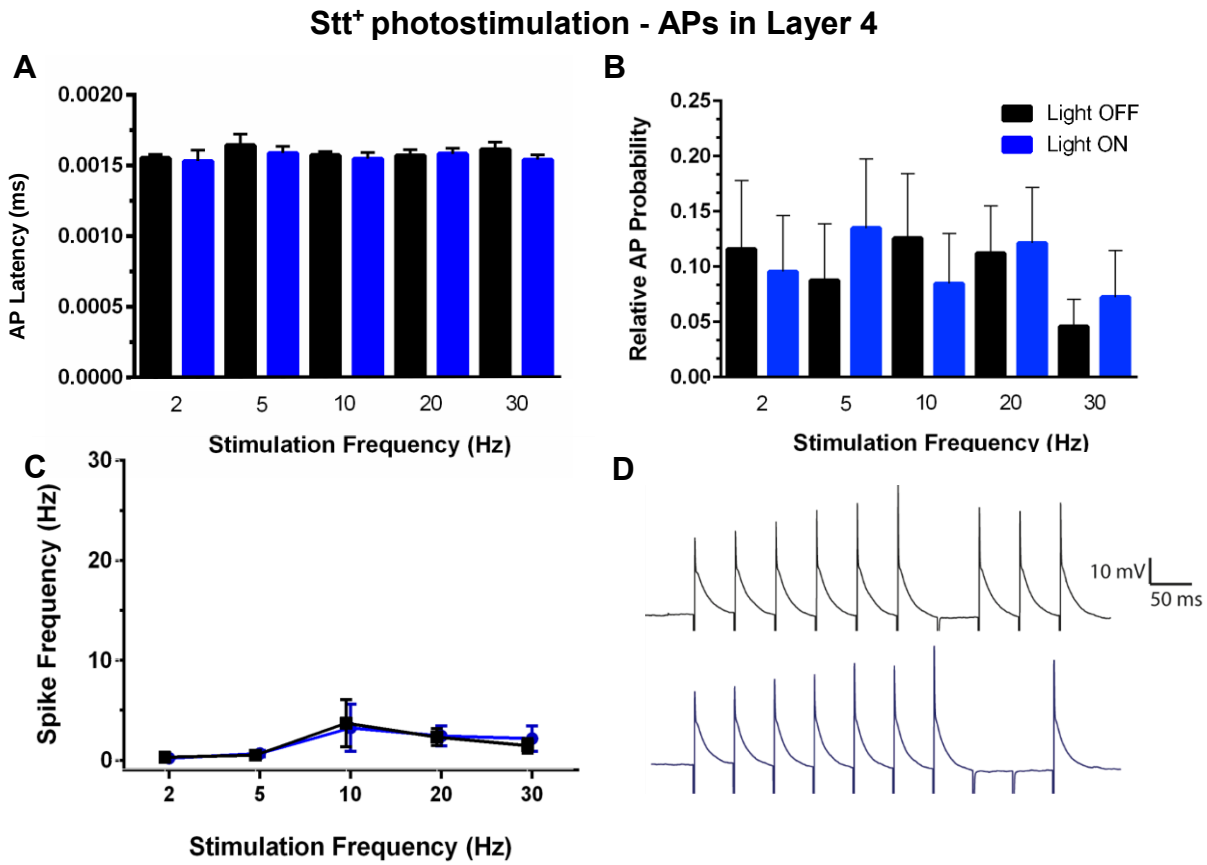

Figure 3.13. Stt⁺ INs optogenetic stimulation does not affect evoked spike frequency in layer 4 of the barrel cortex. Thalamocortical stimulation responses were recorded using ten electric stimulation protocols with 5 different frequencies (2, 5, 10, 20 and 30 Hz) in thalamocortical brain slices of Stt⁺-Cre mice injected with double-floxed inverted hChR2, 4 to 6 weeks after injections. Recordings were also performed in combination with optogenetic stimulation in half of the trials. **(A)** Action potentials (APs) latency (ms), **(B)** probability and **(C)** frequency were measured and compared between optogenetic stimulation and control conditions. Data was grouped by frequency and condition. Represented is mean ± SEM, n=8 cells; there were no statically significant comparisons. Data was analysed with parametric statistical test one-way ANOVA and multicomparisons corrected using with Sidak's multiple comparisons test. **(D)** Example of evoked AP traces at 10 Hz in light ON and light OFF conditions.

In summary, optogenetic stimulation of PV⁺ INs does not have an effect in evoked EPSPs reduces evoked action potential frequency in both layers 4 and 2/3 of the barrel cortex. On other hand, the effect of Stt⁺ INs activation effect on both evoked EPSPs and action potentials is not consistent across stimulation firing frequencies.

3.3 Effect of PV+ INs photostimulation on neural activity *in vivo*

Neurons in layer 2/3 of the barrel cortex receive inputs from layer 4 during somatosensory processing (Bastos et al., 2012). Calcium imaging experiments *in vivo* were performed in order to evaluate the effect of the optogenetic activation of PV+ INs in the processing of sensory information. Layer 2/3 neurons are highly discriminative during whisker-mediated stimulation (O'Connor et al., 2010). Thus, I recorded neuronal network activity in L2/3 during optogenetic and whisker-mediated sensory stimulation, in head-fixed lightly anaesthetised mice, through a cranial glass window with a field of view of 250x250 μm. These mice were previously injected with a mix of virus containing GCaMP6f under control of the synapsin-1 promotor and double-floxed inverted hChR2 under control of EF1α.

Two recordings time windows in each experiment condition were analysed and compared with each other (Figure 2.7). As a control for further measurements, activity from a window right after the beginning of the recording (Ctrl–C1) was compared with activity from a recording window towards the 30 s measurement (Ctrl–C2; Figure 3.14). Difference between the two is non-significant; n=22.

With the purpose of assessing the relative contribution of PV+ INs on spontaneous neural network activity, PV+ neurons expressing ChR2 were activated by photostimulation immediately before imaging. The first seven seconds of activity after optogenetic stimulation (Opto.–O) were compared with a control window measured towards the end of the 30 s recording (Opto.–C; Figure 3.14). I observed a significant increase, 240% ($p<0.0001$, n=22), of relative fluorescence following optogenetic stimulation of PV+ INs.

In order to confirm that the field of view imaged included neurons that were indeed barrels involved in the processing of somatosensory stimuli, I assessed the effect of contralateral whisker-mediated sensory stimulation on network activity on this layer. The relative change in fluorescence between an initial control recording window (Stim.–C) was compared with a period in which whiskers were deflected (Stim.–S; Figure 3.14). Sensory stimulation increased network activity by 170% ($p<0.0001$, n=13).

Finally, to evaluate the effect of PV+ optogenetic stimulation on the processing of whisker-mediated sensory information, photostimulation immediately before the

initial recording window was combined with sensory stimulation of contralateral whiskers. A significant increase of 210% ($p<0.0001$, $n=10$) in relative change in fluorescence was observed when an initial seven seconds recording window (Opto_Stim. –O+S) was compared with a 7 seconds later window in which whisker were being deflected (Opto_Stim.–S; Figure 3.14)

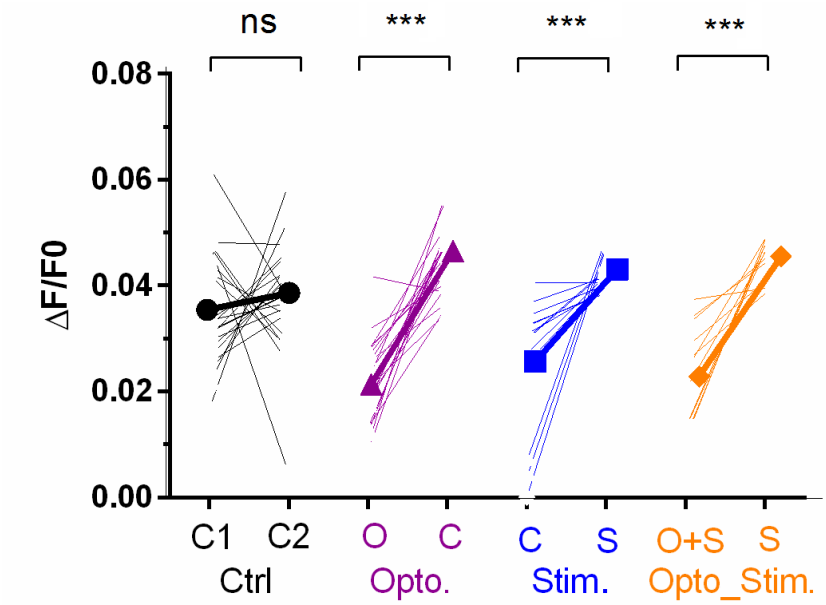

Figure 3.14. Network activity in layer 2/3 of the barrel cortex is decreased by optogenetic stimulation of PV⁺ INs and increased by whisker-mediated sensory stimulation. 2 to 4 weeks after adult mice injections with a mix of virus containing GCaMP6f under synapsin-promotor and double-floxed inverted hChR2, a head bar and a glass cranial window were implanted in the mice skull. Two-photon calcium-imaging experiments were performed in anaesthetized mice in control (**Ctrl**), optogenetic stimulation (**Opto.**), whisker-mediated sensory stimulation (**Stim.**) or optogenetic and sensory stimulation (**Opto_Stim.**) conditions. Represented is the relative change in fluorescence (**ΔF/F0**), in layer 2/3 of the barrel cortex between two distinct recording windows in each condition. Each line represents an individual 30 s measurement and thicker lines with shapes represent condition means. Values obtained were analysed with Sidak's multiple comparisons test. **Ns** – non-significant; *** - p<0. 0001.

These results show that photostimulation of PV⁺ neurons reduces spontaneous network activity of neurons in layer 2/3 of the barrel cortex of lightly anaesthetized mice. As illustrated in the representative calcium trace of Figure 3.15, optogenetic stimulation is able to decrease spontaneous neuronal network spontaneous activity for up to three seconds.

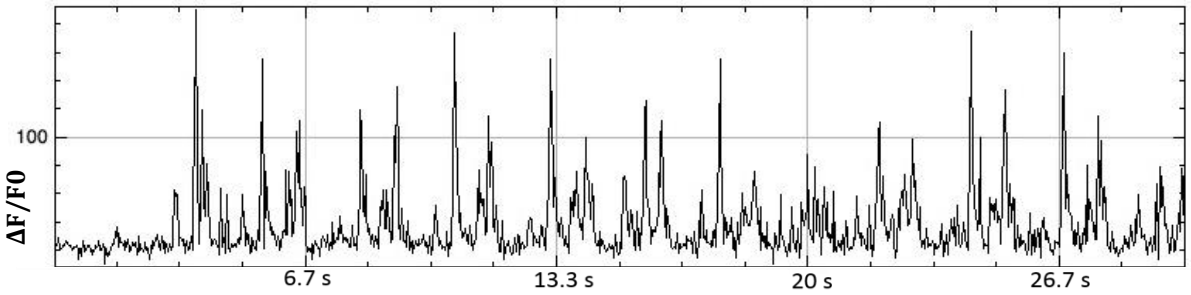

Figure 3.15. Spontaneous activity of neurons in layer 2/3 of the barrel cortex is decreased by optogenetic stimulation of PV⁺ INs neurons during ~3 s. Example calcium-imaging trace of a single neuron in layer 2/3 of the barrel cortex recorded after optogenetic stimulation of PV⁺ neurons in PV⁺-Cre mice injected with a mix of virus containing GCaMP6f under synapsin-promotor and double-floxed inverted hChR2. Plotted is the mean relative fluorescence per time (s).

Furthermore, optogenetic stimulation of PV⁺ neurons is able to decrease whisker-mediated evoked activity in layer 2/3 of the mouse barrel cortex in lightly anaesthetized mice.

Marta Huelin Gorriz, Erasmus⁺ student from the Master of Science in Neurosciences, Vrije University of Amsterdam (The Netherlands) contributed to electrophysiology data and collaborated on *in vivo* experiments presented in this chapter.

.

Chapter IV

Discussion

4.1 ChR2 and GCaMP6f as an optogenetic approach for INs cell-type specific activity manipulation and recording of neural activity

In order to enable selective manipulation of PV^+ and Stt^+ INs populations, I devised an optogenetic approach. Channelrhodopsin 2, a light-gated non-selective cationic membrane channel, was chosen as it is able to depolarize neurons in which it is expressed allowing a precise activity control with high temporal resolution by simple illumination on the appropriate wavelength (470 nm) (Nagel et al., 2003). Versions of this opsin containing the human synapsin 1 promoter, so called 'humanized', were selected for their enhanced expression in mammals (Boyden et al., 2005). Taking into consideration the activation properties of fast-spiking and PV^+ and slow-adapting Stt^+ interneurons, I selected variants of channelrodopsin2 with different activity kinetics. While in Stt^+-Cre mice I injected the commonly used version of ChR2, to activate PV^+ INs I used a ChR2 variant, ChETA, with faster deactivation kinetics, which would allow me to use activate PV+ neurons with high fidelity even at very high frequencies (up to 200 Hz).

Therefore, the first step of this project was the establishment of homozygous mouse transgenic colonies that expressed the Cre enzyme under the promoter of parvalbumin or somatostatin. Then, viruses containing the appropriate opsins coupled to fluorescent proteins, double-floxed and inverted in the respective vectors were injected in those transgenic mice. The expression of the fluorescent proteins observed in the respective immunohistochemistry results confirmed the success of the cre-mediated recombination in the interneurons of interest in the mouse barrel cortex of both, PV^+ and Stt^+-Cre, transgenic trains (Figure 3.2).

In the future, additional experiments may be performed to have a better quantification of the effect of these optogenetic actuators in the respective interneurons and associated microcircuit. In order to do this, I will obtain current-clamp recordings from infected cells. Possible complications of this step are the low percentage of inhibitory neurons in cortical layers (Fino and Yuste, 2011) and the sparse infection of the virus used when injected in neonates (~50%). Additionally, voltage-clamp recordings from cells that receive inputs from a

putative optogenetically infected cell will allow a better characterization of the effect of specific interneurons optogenetic stimulation in connected cells.

In *in vivo* experiments, this approach was combined with non-cell specific expression of the genetically encoded calcium indicator GCaMP6f. Through histology experiments I confirmed the expression of both GCaMP6f and ChR2. Was my objective to record activity in layers 4 and 2/3 of the barrel cortex, however the levels of GCaMP6f in layer 4 were very low (Figure 3.4). Another group also recently reported a GCaMP6 expression issue in layer 4 of the barrel cortex (Peron et al., 2015). In order to overcome this problem in future experiments, transgenic mice which endogenously express GCaMP can be used in combination with cre-lines of interest.

4.2 Distinct role of PV^+ and Stt^+ INs on thalamocortical synaptic transmission

During somatosensory processing, the thalamus works as a relay station of sensory information (Camarillo et al., 2012). Information received in this brain structure is processed and mainly transmitted into layer 4 of the barrel cortex. From here is then relayed into 2/3 (Bastos et al., 2012). To assess the role of PV^+ and Stt^+ interneurons in thalamocortical synaptic transmission I used genetically targeted cell-type specific optogenetic manipulation of IN activity in these layers.

In layer 4, optogenetic stimulation of PV^+ interneurons did not affect evoked excitatory postsynaptic potentials (EPSPs) (Figure 3.9). However, it decreased the action probability of excitatory cells in both layer 4 and 2/3 (Figures 3.10 and 3.11). Although reduction was not statistically significant, it is systematic across the stimulation frequencies used. This reduction in output firing frequency is in accordance with the reported circuit connectivity between PV^+ interneurons and excitatory cells in these layers of the cortex (Holmgren et al., 2003, Pfeffer et al., 2013). In the future, an increase in the number of recordings might allow obtaining statistically more significant differences between light ON and light OFF conditions. Increasing the number of data sets for excitatory cells would also enable a more detailed clustering of different types of excitatory neurons

according to their electrophysiological properties, which should help expand our understating of the local microcircuits.

PV^+ neurons have a very dense connectivity in the cortex and are virtually connected to all the local excitatory neurons (Avermann et al., 2012, Estebanez et al., 2015). Thus, as optogenetic stimulation would most likely mainly bring the membrane potential of these INs closer to the action potential threshold rather than eliciting action potentials, PV^+ neurons would still need to be activated by other cells for this effect to be observable in excitatory cells. Excitatory cells establish feedback connections with PV^+ INs that enervate them (Yoshimura and Callaway, 2005, Hofer et al., 2011, Li et al., 2014). Therefore, PV^+ neurons are more likely to fire only when the excitatory cells with which they establish connections spike. Subsequently, the effect of the PV^+ interneurons optogenetic stimulation here described would only be observable when the excitatory cell from which recordings were obtained displayed action potentials. Thus, the effect of optogenetic stimulation of these INs in excitatory cells action potentials but not in EPSPs is likely to be caused by the feedback loop between PV^+ INs and nearby excitatory cells.

In recordings obtained from cells in layer 2/3, it was not possible to observe EPSPs but only action potentials (Figure 3.11). This all-or-none response to stimulation in the internal capsule might be caused by the methodology. Unlike layer 4, layer 2/3 do not directly receives thalamic inputs (Bastos et al., 2012). Additionally, transmission from L4 to L2/3 has a high threshold and requires the activation of many layer 4 neurons (Feldmeyer et al., 2002). Consequently, applied electrical stimulation in the internal capsule required much higher intensities in order to obtain evoked-responses in layer 2/3 (20 to 300 μA in layer 4 and 4 to 11 mA in layer 2/3). When induced electric stimulation is higher than 320 μA, the finer adjustment allowed by the used isolated stimulator is ~100 μA. Therefore, it likely that, in order to record EPSPs responses in layer 2/3 I need a finer adjustment of stimulation that would allow me to evoke subthreshold responses. Thus, in future experiments, placing the stimulation electrode in thalamocortical projections closer to layer 2/3 might reduce the necessary electric stimulation, allowing a finer regulation.

Optogenetic stimulation of Stt$^+$ interneurons did not have a consistent effect in both EPSPs (Figure 3.12) and action potentials (Figure 3.13) of excitatory cells recorded in layer 4. Unlike PV$^+$ neurons, which have a very dense connectivity with local excitatory cells, Stt$^+$ INs in this layer preferentially inhibit PV$^+$ interneurons (Cottam et al., 2013, Xu et al., 2013). Therefore, a direct effect of Stt$^+$ INs photostimulation on excitatory cells in these layers is not expected.

Moreover, in layer 4, thalamocortical stimulation strongly stimulate PV$^+$ interneurons but has a very week effect in Stt$^+$ INs (Beierlein et al., 2003). Thus, considering that Stt$^+$ do not directly target excitatory cells, but instead have a desinhibition effect by synapsing with PV$^+$ neurons(Cottam et al., 2013), the effect of Stt$^+$ INs photostimulation might be masked by the increased thalamocortical PV$^+$ INs inhibition during our electric stimulation protocols. This could be assessed in future experiments by also recording activity also from PV$^+$ interneurons during photostimulation of Stt$^+$ INs.

Additionally, Stt$^+$ INs require a sustained activation and have a slower longer-lasting activation with less fine temporal regulation than PV$^+$ interneurons (Pala and Petersen, 2015). Hence, in future experiments, in order to accurately assess the effect of Stt$^+$ INs in excitatory cells of layer 4, I will use stimulation protocols with longer periods of photostimulation.

4.3 Role of PV$^+$ INs in somatosensory processing

Neurons in layer 2/3 of the barrel cortex receive inputs from layer 4 during somatosensory processing (Bastos et al., 2012). Additionally, layer 2/3 neurons are highly discriminative during whisker-mediated stimulation (O'Connor et al., 2010). Electrophysiology results suggest that PV$^+$ increased activity in thalamocortical transmission decreases the activity of excitatory cells layers 4 and 2/3 of the barrel cortex. Therefore, I delineated *in vivo* experiments to complement and better understand my electrophysiological results in the light of somatosensory processing. In order to study the role of PV$^+$ interneurons in the processing of somatosensory sensory information in neural populations, I recorded changes in neural activity in layer 2/3 of the barrel cortex during whisker-mediated stimulation, using optogenetic stimulation combined with calcium imaging experiments.

The non-significant changes in activity in the control condition (Figure 3.14) validated the statistically significant results observed in conditions with optogenetic and/or sensory stimulation. The significant 240 % decrease of relative fluorescence with optogenetic stimulation revealed the capacity of PV^+ INs photostimulation to inhibit spontaneous neural activity (Figures 3.14 and 3.15).

Whisker stimulation is processed in the barrel cortex by cortical columns organized in the same layout as the whiskers in the snout (Diamond et al., 2008). Thus, inputs receive in L4 of the barrel cortex have receptive field limitations, which in turn are reflected in L2/3 activity due to columnar transmission restrictions (Quairiaux et al., 2007). However, the significant 170% increase in activity during stimulation of contralateral whiskers validates the connectivity between the stimulated whiskers and the barrel cortex areas in which calcium imaging recordings were performed (Figure 3.14).

Finally, it was observed that increased PV^+ INs optogenetic activity has the capacity to significantly (210%) decrease whisker-mediated neural activity in layer 2/3 (Figure 3.14). Although the optogenetic reporter used here was expressed in a cell-type specific fashion, excitatory neurons account for the vast majority of neurons in cortex (Ascoli et al., 2008). Thus, and considering the huge decrease in activity observed, the change of relative fluorescence observed likely represent a decrease in excitatory cells activity.

These results are in accordance with the dense connectivity between PV+ interneurons and excitatory cells (Avermann et al., 2012, Estebanez et al., 2015). And with the reduced activity in L2/3 excitatory cells observed in electrophysiology recordings during thalamocortical inhibition. Several reasons can explain the different significances of activity reduction observed in the two experiments. The *in vivo* experiments compensate for differences in aCSF/CSF ionic concentrations and for any long-range synaptic connectivity and neuromodulation effects lost in brain slices used in *in vitro* electrophysiological experiments. Additionally, in two-photo calcium imaging experiment I recorded the activity of a significantly higher number of cells, looking at neural populations rather than single cell level effect. Finally, virus stereotaxic injections for electrophysiology experiments were performed in neonates while for two-photon

calcium imaging I injected adult animals. Therefore, the levels of expression of ChR2 in the two experiments might be significantly different, thus impacting the level of PV^+ optogenetic stimulation effect between the two conditions. This could be assed by quantifying the expression observed in the two experiments and try to compensate for the physiological differences of the injections by adjusting virus concentrations.

When considering the differences between activity changes across conditions, it is possible to note that change in activity following optogenetic stimulation of PV^+ neurons are higher in spontaneous activity than in sensory processing stimulation conditions. This could suggest that applied optogenetic stimulation of PV^+ neurons is not sufficient to inhibit in the same degree excitatory cells, which could occur because of intracortical feedforward networks altered during the processing of sensory stimuli.

Alternatively, these results could mean that during whisker-mediated stimuli, other types of cells, which are not directly inhibited by PV^+ INs activation, are active, as the excitatory ones. Stt^+ neurons would be very good candidates as they are not directly inhibited by PV^+ INs. Instead, Stt^+ neurons are activated by sensory stimuli and inhibit PV^+ neurons during sensory processing (Cottam et al., 2013), thus, having the potential to reduce the change in fluorescence activity.

A third explanation for these differences could be related with the reported increase in PV^+ INs activity during sensory stimulation in order to improve receptive field and discrimination, as observed in the visual system (Lee et al., 2012). Therefore, during whisker-mediated sensory stimulation the activity of PV^+ INs could be already increased, which would slightly reduce the prominent effect of the optogenetic stimulation of these neurons on the activity of the neuronal network.

In order to better understand the importance of an increased PV^+ activation in sensory processing and its effects on specific cell types in layer 2/3, I would perform two-photon calcium imaging experiments with cell-type and or layer specific expression of GCaMP6f and ChR2. A similar approach could also be used to assess the effect of sensory stimulation itself on changes of activity of specific INs. For more precise measurements, calcium-imaging experiments could be combined with *in vivo* electrophysiology.

Additionally, combining PV^+ INs optogenetic photostimulation with sensory discrimination tasks in head-fixed awake behaving animals could help assess the physiological meaning of these relative network activity alterations.

Chapter V

Conclusion

In this project I validated an optogenetic approach to dissect the role of inhibitory neurons in sensory processing. This approach combines the cell-type specific expression of optogenetic actuators with the expression of optogenetic reporters. I used this to dissociate the role of specific interneurons in synaptic transmission *in vitro* and sensory processing *in vivo* in the mouse barrel cortex. This methodological approach will, therefore, be of great value to study the role of interneurons on E/I balance maintenance, hypothesised as essential in the processing of sensory information.

Results obtained *in vitro* revealed a distinct role on the inhibition provided by Stt^+ and PV^+ inhibitory neurons during synaptic transmission of thalamic inputs into the barrel cortex. This is in accordance with my initial hypothesis that cortical inhibitory subpopulations have distinct roles in maintaining the balance between excitation and inhibition during sensory processing of information.

Moreover, *in vivo* two-photon calcium imaging experiments strongly support the close relation between PV^+ INs and excitatory cells observed in electrophysiological results. I observed a prominent effect of PV^+ INs photostimulation on networks of neurons crucial in the integration of sensory information during somatosensory processing. This is line with previous studies in different sensory systems, which point out the relevance of PV^+ neuronal activity for sharpening of the sensory receptive field (Lee et al., 2012).

The study of the role of specific INs populations in somatosensory processing and its correlation with perception will help us to elucidate hypothesised sensory coding principles. This can later be achieved *in vivo* by combining sensory inputs with motor responses and learning processes in awake, behaving animals, hence directly relating neuronal activity with behaviour (Ferezou et al., 2007, Cascio, 2010, Huber et al., 2012).

References

Adrian ED, Zotterman Y (1926) The impulses produced by sensory nerve-endings: Part II. The response of a Single End-Organ. J Physiol 61:151-171.

Agmon A, Connors BW (1991) Thalamocortical responses of mouse somatosensory (barrel) cortex in vitro. Neuroscience 41:365-379.

Ahissar E, Sosnik R, Bagdasarian K, Haidarliu S (2001) Temporal frequency of whisker movement. II. Laminar organization of cortical representations. Journal of neurophysiology 86:354-367.

Ahissar E, Sosnik R, Haidarliu S (2000) Transformation from temporal to rate coding in a somatosensory thalamocortical pathway. Nature 406:302-306.

Arabzadeh E, Panzeri S, Diamond ME (2006) Deciphering the spike train of a sensory neuron: counts and temporal patterns in the rat whisker pathway. The Journal of Neuroscience 26:9216-9226.

Arabzadeh E, Zorzin E, Diamond ME (2005) Neuronal encoding of texture in the whisker sensory pathway. PLoS biology 3:e17.

Ascoli GA, Alonso-Nanclares L, Anderson SA, Barrionuevo G, Benavides-Piccione R, Burkhalter A, Buzsaki G, Cauli B, Defelipe J, Fairen A, Feldmeyer D, Fishell G, Fregnac Y, Freund TF, Gardner D, Gardner EP, Goldberg JH, Helmstaedter M, Hestrin S, Karube F, Kisvarday ZF, Lambolez B, Lewis DA, Marin O, Markram H, Munoz A, Packer A, Petersen CC, Rockland KS, Rossier J, Rudy B, Somogyi P, Staiger JF, Tamas G, Thomson AM, Toledo-Rodriguez M, Wang Y, West DC, Yuste R (2008) Petilla terminology: nomenclature of features of GABAergic interneurons of the cerebral cortex. Nat Rev Neurosci 9:557-568.

Averbeck BB, Latham PE, Pouget A (2006) Neural correlations, population coding and computation. Nature reviews Neuroscience 7:358-366.

Avermann M, Tomm C, Mateo C, Gerstner W, Petersen CC (2012) Microcircuits of excitatory and inhibitory neurons in layer 2/3 of mouse barrel cortex. Journal of neurophysiology 107:3116-3134.

Bale MR, Campagner D, Erskine A, Petersen RS (2015) Microsecond-scale timing precision in rodent trigeminal primary afferents. The Journal of neuroscience : the official journal of the Society for Neuroscience 35:5935-5940.

Barth AL, Poulet JF (2012) Experimental evidence for sparse firing in the neocortex. Trends in neurosciences 35:345-355.

Bastos AM, Usrey WM, Adams RA, Mangun GR, Fries P, Friston KJ (2012) Canonical microcircuits for predictive coding. Neuron 76:695-711.

Beierlein M, Gibson JR, Connors BW (2003) Two dynamically distinct inhibitory networks in layer 4 of the neocortex. J Neurophysiol 90:2987-3000.

Bialek W, Rieke F, de Ruyter van Steveninck RR, Warland D (1991) Reading a neural code. Science 252:1854-1857.

Boyden ES, Zhang F, Bamberg E, Nagel G, Deisseroth K (2005) Millisecond-timescale, genetically targeted optical control of neural activity. Nat Neurosci 8:1263-1268.

Brenner N, Strong SP, Koberle R, Bialek W, de Ruyter van Steveninck RR (2000) Synergy in a neural code. Neural computation 12:1531-1552.

Brette R (2012) Computing with neural synchrony. PLoS computational biology 8:e1002561.

Bruno RM, Sakmann B (2006) Cortex is driven by weak but synchronously active thalamocortical synapses. Science 312:1622-1627.

Cafaro J, Rieke F (2010) Noise correlations improve response fidelity and stimulus encoding. Nature 468:964-967.

Camarillo L, Luna R, Nacher V, Romo R (2012) Coding perceptual discrimination in the somatosensory thalamus. Proceedings of the National Academy of Sciences of the United States of America 109:21093-21098.

Cascio CJ (2010) Somatosensory processing in neurodevelopmental disorders. J Neurodev Disord 2:62-69.
Cauller L (1995) Layer I of primary sensory neocortex: where top-down converges upon bottom-up. Behavioural brain research 71:163-170.
Chabrol FP, Arenz A, Wiechert MT, Margrie TW, DiGregorio DA (2015) Synaptic diversity enables temporal coding of coincident multisensory inputs in single neurons. Nature neuroscience 18:718-727.
Chen N, Sugihara H, Sur M (2015) An acetylcholine-activated microcircuit drives temporal dynamics of cortical activity. Nat Neurosci 18:892-902.
Connor CE, Johnson KO (1992) Neural coding of tactile texture: comparison of spatial and temporal mechanisms for roughness perception. The Journal of neuroscience : the official journal of the Society for Neuroscience 12:3414-3426.
Cottam JC, Smith SL, Hausser M (2013) Target-specific effects of somatostatin-expressing interneurons on neocortical visual processing. J Neurosci 33:19567-19578.
Cowan AI, Stricker C (2004) Functional connectivity in layer IV local excitatory circuits of rat somatosensory cortex. Journal of neurophysiology 92:2137-2150.
D'Argembeau A, Jeunehomme O, Majerus S, Bastin C, Salmon E (2014) The Neural Basis of Temporal Order Processing in Past and Future Thought. Journal of cognitive neuroscience 1-13.
de Kock CP, Bruno RM, Spors H, Sakmann B (2007) Layer- and cell-type-specific suprathreshold stimulus representation in rat primary somatosensory cortex. The Journal of physiology 581:139-154.
deCharms RC, Zador A (2000) Neural representation and the cortical code. Annual review of neuroscience 23:613-647.
Deschênes M, Timofeeva E, Lavallée P, Dufresne C (2005) The vibrissal system as a model of thalamic operations. Progress in brain research 149:31-40.
Diamond ME (2000) Neurobiology. Parallel sensing. Nature 406:245, 247.
Diamond ME (2010) Texture sensation through the fingertips and the whiskers. Current opinion in neurobiology 20:319-327.
Diamond ME, von Heimendahl M, Knutsen PM, Kleinfeld D, Ahissar E (2008) 'Where' and 'what' in the whisker sensorimotor system. Nat Rev Neurosci 9:601-612.
Dimitrov AG, Miller JP (2001) Neural coding and decoding: communication channels and quantization. Network 12:441-472.
Eggermont JJ (1998) Is there a neural code? Neuroscience and biobehavioral reviews 22:355-370.
Estebanez L, Kremkow J, Poulet JF (2015) Matching Cell Type to Function in Cortical Circuits. Neuron 87:249-251.
Feldmeyer D, Lubke J, Silver RA, Sakmann B (2002) Synaptic connections between layer 4 spiny neurone-layer 2/3 pyramidal cell pairs in juvenile rat barrel cortex: physiology and anatomy of interlaminar signalling within a cortical column. J Physiol 538:803-822.
Ferezou I, Haiss F, Gentet LJ, Aronoff R, Weber B, Petersen CC (2007) Spatiotemporal dynamics of cortical sensorimotor integration in behaving mice. Neuron 56:907-923.
Fino E, Yuste R (2011) Dense inhibitory connectivity in neocortex. Neuron 69:1188-1203.
Foeller E, Celikel T, Feldman DE (2005) Inhibitory sharpening of receptive fields contributes to whisker map plasticity in rat somatosensory cortex. Journal of neurophysiology 94:4387-4400.
Friston KJ (1997) Another neural code? NeuroImage 5:213-220.
Gabernet L, Jadhav SP, Feldman DE, Carandini M, Scanziani M (2005) Somatosensory integration controlled by dynamic thalamocortical feed-forward inhibition. Neuron 48:315-327.
Galindo-Leon EE, Lin FG, Liu RC (2009) Inhibitory plasticity in a lateral band improves cortical detection of natural vocalizations. Neuron 62:705-716.
Gautrais J, Thorpe S (1998) Rate coding versus temporal order coding: a theoretical approach. Bio Systems 48:57-65.

Gerstner W, Kreiter AK, Markram H, Herz AV (1997) Neural codes: firing rates and beyond. Proceedings of the National Academy of Sciences of the United States of America 94:12740-12741.

Ghazanfar AA, Nicolelis MA (1997) Nonlinear processing of tactile information in the thalamocortical loop. Journal of neurophysiology 78:506-510.

Graham DJF, D. J. (2007) Sparse Coding in the Neocortex. Evolution of Nervous Systems III:181-187.

Haider B, Hausser M, Carandini M (2013) Inhibition dominates sensory responses in the awake cortex. Nature 493:97-100.

Hausser M, Smith SL (2007) Neuroscience: controlling neural circuits with light. Nature 446:617-619.

Hipp J, Arabzadeh E, Zorzin E, Conradt J, Kayser C, Diamond ME, Konig P (2006) Texture signals in whisker vibrations. Journal of neurophysiology 95:1792-1799.

Hofer SB, Ko H, Pichler B, Vogelstein J, Ros H, Zeng H, Lein E, Lesica NA, Mrsic-Flogel TD (2011) Differential connectivity and response dynamics of excitatory and inhibitory neurons in visual cortex. Nat Neurosci 14:1045-1052.

Holmgren C, Harkany T, Svennenfors B, Zilberter Y (2003) Pyramidal cell communication within local networks in layer 2/3 of rat neocortex. J Physiol 551:139-153.

Huber D, Gutnisky DA, Peron S, O'Connor DH, Wiegert JS, Tian L, Oertner TG, Looger LL, Svoboda K (2012) Multiple dynamic representations in the motor cortex during sensorimotor learning. Nature 484:473-478.

Jacobs AL, Fridman G, Douglas RM, Alam NM, Latham PE, Prusky GT, Nirenberg S (2009) Ruling out and ruling in neural codes. Proceedings of the National Academy of Sciences of the United States of America 106:5936-5941.

Jadhav SP, Wolfe J, Feldman DE (2009) Sparse temporal coding of elementary tactile features during active whisker sensation. Nature neuroscience 12:792-800.

Jaeger D (2007) Pauses as neural code in the cerebellum. Neuron 54:9-10.

Johansson RS, Birznieks I (2004) First spikes in ensembles of human tactile afferents code complex spatial fingertip events. Nature neuroscience 7:170-177.

Jones LM, Lee S, Trageser JC, Simons DJ, Keller A (2004) Precise temporal responses in whisker trigeminal neurons. Journal of neurophysiology 92:665-668.

Kjaer TW, Hertz JA, Richmond BJ (1994) Decoding cortical neuronal signals: network models, information estimation and spatial tuning. Journal of computational neuroscience 1:109-139.

Koyama S (2012) On the relation between encoding and decoding of neuronal spikes. Neural computation 24:1408-1425.

Kumar A, Rotter S, Aertsen A (2010) Spiking activity propagation in neuronal networks: reconciling different perspectives on neural coding. Nature reviews Neuroscience 11:615-627.

Lee SH, Kwan AC, Zhang S, Phoumthipphavong V, Flannery JG, Masmanidis SC, Taniguchi H, Huang ZJ, Zhang F, Boyden ES, Deisseroth K, Dan Y (2012) Activation of specific interneurons improves V1 feature selectivity and visual perception. Nature 488:379-383.

Leiser SC, Moxon KA (2007) Responses of trigeminal ganglion neurons during natural whisking behaviors in the awake rat. Neuron 53:117-133.

Lewis DA, Hashimoto T, Volk DW (2005) Cortical inhibitory neurons and schizophrenia. Nature reviews Neuroscience 6:312-324.

Li LY, Ji XY, Liang F, Li YT, Xiao Z, Tao HW, Zhang LI (2014) A feedforward inhibitory circuit mediates lateral refinement of sensory representation in upper layer 2/3 of mouse primary auditory cortex. J Neurosci 34:13670-13683.

London M, Roth A, Beeren L, Hausser M, Latham PE (2010) Sensitivity to perturbations in vivo implies high noise and suggests rate coding in cortex. Nature 466:123-127.

Lopez de Armentia M, Sah P (2004) Firing properties and connectivity of neurons in the rat lateral central nucleus of the amygdala. J Neurophysiol 92:1285-1294.

Luo L, Callaway EM, Svoboda K (2008) Genetic dissection of neural circuits. Neuron 57:634-660.

Lynn B (1975) Somatosensory receptors and their CNS connections. Annual review of physiology 37:105-127.

Mateo C, Avermann M, Gentet LJ, Zhang F, Deisseroth K, Petersen CC (2011) In vivo optogenetic stimulation of neocortical excitatory neurons drives brain-state-dependent inhibition. Current biology : CB 21:1593-1602.

Mauk MD, Buonomano DV (2004) The neural basis of temporal processing. Annual review of neuroscience 27:307-340.

Metcalfe JS, McDowell K, Chang TY, Chen LC, Jeka JJ, Clark JE (2005) Development of somatosensory-motor integration: an event-related analysis of infant posture in the first year of independent walking. Developmental psychobiology 46:19-35.

Middlebrooks JC, Clock AE, Xu L, Green DM (1994) A panoramic code for sound location by cortical neurons. Science 264:842-844.

Miller JP (1994) Neural coding. Neurons cleverer than we thought? Current biology : CB 4:818-820.

Miyashita T, Feldman DE (2013) Behavioral detection of passive whisker stimuli requires somatosensory cortex. Cerebral cortex 23:1655-1662.

Moore CI, Carlen M, Knoblich U, Cardin JA (2010) Neocortical interneurons: from diversity, strength. Cell 142:189-193.

Moore CI, Nelson SB (1998) Spatio-temporal subthreshold receptive fields in the vibrissa representation of rat primary somatosensory cortex. Journal of neurophysiology 80:2882-2892.

Nagel G, Szellas T, Huhn W, Kateriya S, Adeishvili N, Berthold P, Ollig D, Hegemann P, Bamberg E (2003) Channelrhodopsin-2, a directly light-gated cation-selective membrane channel. Proceedings of the National Academy of Sciences of the United States of America 100:13940-13945.

Nicolelis MA, Ribeiro S (2006) Seeking the neural code. Scientific American 295:70-77.

Nowotny T, Huerta R, Rabinovich MI (2008) Neuronal synchrony: peculiarity and generality. Chaos 18:037119.

O'Connor DH, Hires SA, Guo ZV, Li N, Yu J, Sun QQ, Huber D, Svoboda K (2013) Neural coding during active somatosensation revealed using illusory touch. Nat Neurosci 16:958-965.

O'Connor DH, Huber D, Svoboda K (2009) Reverse engineering the mouse brain. Nature 461:923-929.

O'Connor DH, Peron SP, Huber D, Svoboda K (2010) Neural activity in barrel cortex underlying vibrissa-based object localization in mice. Neuron 67:1048-1061.

Okun M, Lampl I (2008) Instantaneous correlation of excitation and inhibition during ongoing and sensory-evoked activities. Nature neuroscience 11:535-537.

Olshausen BA, Field DJ (2004) Sparse coding of sensory inputs. Current opinion in neurobiology 14:481-487.

Ostojic S (2011) Interspike interval distributions of spiking neurons driven by fluctuating inputs. Journal of neurophysiology 106:361-373.

Packer AM, Roska B, Hausser M (2013) Targeting neurons and photons for optogenetics. Nature neuroscience 16:805-815.

Packer AM, Yuste R (2011) Dense, unspecific connectivity of neocortical parvalbumin-positive interneurons: a canonical microcircuit for inhibition? The Journal of neuroscience : the official journal of the Society for Neuroscience 31:13260-13271.

Pala A, Petersen CC (2015) In vivo measurement of cell-type-specific synaptic connectivity and synaptic transmission in layer 2/3 mouse barrel cortex. Neuron 85:68-75.

Panzeri S, Petersen RS, Schultz SR, Lebedev M, Diamond ME (2001) The role of spike timing in the coding of stimulus location in rat somatosensory cortex. Neuron 29:769-777.

Panzeri S, Petroni F, Petersen RS, Diamond ME (2003) Decoding neuronal population activity in rat somatosensory cortex: role of columnar organization. Cerebral cortex 13:45-52.

Peron SP, Freeman J, Iyer V, Guo C, Svoboda K (2015) A Cellular Resolution Map of Barrel Cortex Activity during Tactile Behavior. Neuron 86:783-799.

Perona P (2014) Quantized response times are a signature of a neuronal bottleneck in decision. Frontiers in computational neuroscience 8:42.
Petersen CC (2007) The functional organization of the barrel cortex. Neuron 56:339-355.
Petersen CC (2009) Genetic manipulation, whole-cell recordings and functional imaging of the sensorimotor cortex of behaving mice. Acta physiologica 195:91-99.
Petersen RS, Panzeri S, Diamond ME (2002a) Population coding in somatosensory cortex. Current opinion in neurobiology 12:441-447.
Petersen RS, Panzeri S, Diamond ME (2002b) The role of individual spikes and spike patterns in population coding of stimulus location in rat somatosensory cortex. Bio Systems 67:187-193.
Pfeffer CK, Xue M, He M, Huang ZJ, Scanziani M (2013) Inhibition of inhibition in visual cortex: the logic of connections between molecularly distinct interneurons. Nat Neurosci 16:1068-1076.
Pinto DJ, Brumberg JC, Simons DJ (2000) Circuit dynamics and coding strategies in rodent somatosensory cortex. Journal of neurophysiology 83:1158-1166.
Pinto L, Dan Y (2015) Cell-Type-Specific Activity in Prefrontal Cortex during Goal-Directed Behavior. Neuron 87:437-450.
Porter R (2004) The biological significance of skin-to-skin contact and maternal odours. Acta Paediatrica 93:1560-1562.
Pouget A, Dayan P, Zemel R (2000) Information processing with population codes. Nature reviews Neuroscience 1:125-132.
Poulet JF, Fernandez LM, Crochet S, Petersen CC (2012) Thalamic control of cortical states. Nature neuroscience 15:370-372.
Quairiaux C, Armstrong-James M, Welker E (2007) Modified sensory processing in the barrel cortex of the adult mouse after chronic whisker stimulation. J Neurophysiol 97:2130-2147.
Ritt JT, Andermann ML, Moore CI (2008) Embodied information processing: vibrissa mechanics and texture features shape micromotions in actively sensing rats. Neuron 57:599-613.
Rubenstein JL, Merzenich MM (2003) Model of autism: increased ratio of excitation/inhibition in key neural systems. Genes, brain, and behavior 2:255-267.
Rudy B, Fishell G, Lee S, Hjerling-Leffler J (2011) Three groups of interneurons account for nearly 100% of neocortical GABAergic neurons. Dev Neurobiol 71:45-61.
Sachidhanandam S, Sreenivasan V, Kyriakatos A, Kremer Y, Petersen CC (2013) Membrane potential correlates of sensory perception in mouse barrel cortex. Nature neuroscience 16:1671-1677.
Scanziani M, Hausser M (2009) Electrophysiology in the age of light. Nature 461:930-939.
Schneidman E, Puchalla JL, Segev R, Harris RA, Bialek W, Berry MJ, 2nd (2011) Synergy from silence in a combinatorial neural code. The Journal of neuroscience : the official journal of the Society for Neuroscience 31:15732-15741.
Sejnowski TJ (1995) Time for a new neural code? Nature 376:21-22.
Shadlen MN, Newsome WT (1994) Noise, neural codes and cortical organization. Current opinion in neurobiology 4:569-579.
Shoykhet M, Doherty D, Simons DJ (2000) Coding of deflection velocity and amplitude by whisker primary afferent neurons: implications for higher level processing. Somatosensory & motor research 17:171-180.
Singer W (1999) Neuronal synchrony: a versatile code for the definition of relations? Neuron 24:49-65, 111-125.
Sohal VS, Zhang F, Yizhar O, Deisseroth K (2009) Parvalbumin neurons and gamma rhythms enhance cortical circuit performance. Nature 459:698-702.
Spruston N (2008) Pyramidal neurons: dendritic structure and synaptic integration. Nat Rev Neurosci 9:206-221.
Stanley GB (2013) Reading and writing the neural code. Nature neuroscience 16:259-263.

Steuber V, Mittmann W, Hoebeek FE, Silver RA, De Zeeuw CI, Hausser M, De Schutter E (2007) Cerebellar LTD and pattern recognition by Purkinje cells. Neuron 54:121-136.

Stevens CF, Zador A (1995) Neural coding: The enigma of the brain. Current biology : CB 5:1370-1371.

Sturgill JF, Isaacson JS (2015) Somatostatin cells regulate sensory response fidelity via subtractive inhibition in olfactory cortex. Nature neuroscience 18:531-535.

Theunissen F, Miller JP (1995) Temporal encoding in nervous systems: a rigorous definition. Journal of computational neuroscience 2:149-162.

Thevenaz P, Ruttimann UE, Unser M (1998) A pyramid approach to subpixel registration based on intensity. IEEE Trans Image Process 7:27-41.

Thorpe S, Delorme A, Van Rullen R (2001) Spike-based strategies for rapid processing. Neural networks : the official journal of the International Neural Network Society 14:715-725.

Thorpe SJ, Gautrais J (1997) Rapid visual processing using spike asynchrony. Advances in neural information processing systems 901-907.

Trachtenberg JT (2015) Parvalbumin Interneurons: All Forest, No Trees. Neuron 87:247-248.

van Vreeswijk C, Sompolinsky H (1996) Chaos in neuronal networks with balanced excitatory and inhibitory activity. Science 274:1724-1726.

VanRullen R, Guyonneau R, Thorpe SJ (2005) Spike times make sense. Trends in neurosciences 28:1-4.

Veinante P, Jacquin MF, Deschênes M (2000) Thalamic projections from the whisker-sensitive regions of the spinal trigeminal complex in the rat. Journal of Comparative Neurology 420:233-243.

Vogels TP, Abbott L (2009) Gating multiple signals through detailed balance of excitation and inhibition in spiking networks. Nature neuroscience 12:483-491.

Vogels TP, Sprekeler H, Zenke F, Clopath C, Gerstner W (2011) Inhibitory plasticity balances excitation and inhibition in sensory pathways and memory networks. Science 334:1569-1573.

von Heimendahl M, Itskov PM, Arabzadeh E, Diamond ME (2007) Neuronal activity in rat barrel cortex underlying texture discrimination. PLoS biology 5:e305.

Wang HP, Spencer D, Fellous JM, Sejnowski TJ (2010) Synchrony of thalamocortical inputs maximizes cortical reliability. Science 328:106-109.

Waxman SG (2010) Clinical neuroanatomy. New York: McGraw-Hill Medical.

Wiggins IM, Hartley DE (2015) A synchrony-dependent influence of sounds on activity in visual cortex measured using functional near-infrared spectroscopy (fNIRS). PloS one 10:e0122862.

Wilent WB, Contreras D (2005) Dynamics of excitation and inhibition underlying stimulus selectivity in rat somatosensory cortex. Nature neuroscience 8:1364-1370.

Wright J, Yang AY, Ganesh A, Sastry SS, Ma Y (2009) Robust face recognition via sparse representation. IEEE transactions on pattern analysis and machine intelligence 31:210-227.

Xu H, Jeong HY, Tremblay R, Rudy B (2013) Neocortical somatostatin-expressing GABAergic interneurons disinhibit the thalamorecipient layer 4. Neuron 77:155-167.

Yizhar O, Fenno LE, Prigge M, Schneider F, Davidson TJ, O'Shea DJ, Sohal VS, Goshen I, Finkelstein J, Paz JT, Stehfest K, Fudim R, Ramakrishnan C, Huguenard JR, Hegemann P, Deisseroth K (2011) Neocortical excitation/inhibition balance in information processing and social dysfunction. Nature 477:171-178.

Yoshimura Y, Callaway EM (2005) Fine-scale specificity of cortical networks depends on inhibitory cell type and connectivity. Nat Neurosci 8:1552-1559.

Young A, Sun QQ (2009) GABAergic inhibitory interneurons in the posterior piriform cortex of the GAD67-GFP mouse. Cereb Cortex 19:3011-3029.

Zhang Z. SQQ (2011) The balance between excitation and inhibition and functional sensory processing in the somatosensory cortex. Int Rev Neurobiol 97:305-333.